THE JOURNAL OF COMPARATIVE NEUROLOGY 465:205–219 (2003)

$Hprt^{(CAG)146}$ Mice: Age of Onset of Behavioral Abnormalities, Time Course of Neuronal Intranuclear Inclusion Accumulation, Neurotransmitter Marker Alterations, Mitochondrial Function Markers, and Susceptibility to 1-Methyl-4-phenyl-1,2,3,6-tetrahydropyridine

SARA J. TALLAKSEN-GREENE,[1] JARED M. ORDWAY,[2,3] ANDREW B. CROUSE,[2] WALKER S. JACKSON,[2] PETER J. DETLOFF,[2] AND ROGER L. ALBIN[1,4]*

[1]Department of Neurology, University of Michigan, Ann Arbor, Michigan 48109-0585
[2]Department of Biochemistry and Molecular Genetics, University of Alabama at Birmingham, Birmingham, Alabama 35294
[3]Department of Developmental Neurobiology, St. Jude Children's Research Hospital, Memphis, Tennessee 38105
[4]Geriatrics Research, Education, and Clinical Center, Ann Arbor Veterans Affairs Medical Center, Ann Arbor, Michigan 48105

ABSTRACT

We reported previously a model of polyglutamine repeat disorders with insertion of 146 CAG repeats into the murine hypoxanthine phosphoribosyl transferase locus ($Hprt^{(CAG)146}$; Ordway et al. [1997] Cell 91:753–763), which does not normally contain polyglutamine repeats. These mice develop an adult-onset neurologic phenotype of incoordination, involuntary limb clasping, seizures, and premature death. Histologic analysis demonstrates widespread ubiquinated neuronal intranuclear inclusions (NIIs). We now report characterization of the age of onset of behavioral abnormalities, correlated with the time course of occurrence of NIIs in several brain regions, and the occurrence of NIIs in non-neuronal tissues. Onset of behavioral abnormalities occurred at approximately 22 weeks of age. There was variable time course of expression of NIIs in several brain regions. Assessment of several non-neuronal tissues revealed nuclear inclusions in hepatocytes and choroid plexus epithelium. γ-Aminobutyric acid (GABA)/benzodiazepine receptors, dopamine D1-like and D2-like receptors, and type 2 vesicular monoamine transporter (VMAT2) binding sites were assayed before and after the onset of behavioral abnormalities. GABA/benzodiazepine receptors were unchanged either before or after the onset of behavioral abnormalities in any region analyzed, whereas striatal D1-like and D2-like receptors were diminished after but not before the onset of symptoms. Dorsal striatal VMAT2 binding sites were decreased before the onset of behavioral changes. Mitochondrial electron transport chain components were assayed with histochemical methods before and after the onset of behavioral changes. There was no change in behaviorally presymptomatic or symptomatic animals. $Hprt^{(CAG)146}$ mice did not exhibit increased susceptibility to the mitochondrial toxin 1-Methyl-4-phenyl-1,2,3,6-tetrahydropyridine. $Hprt^{(CAG)146}$ mice are a useful model for studying polyglutamine repeat disorders. J. Comp. Neurol. 465:205–219, 2003.

Indexing terms: trinucleotide repeats; spinocerebellar ataxia; polyglutamine; Huntington disease; striatum; cerebellum; substantia nigra

Grant sponsor: National Institutes of Health/Public Health Service; Grant number: PHSNS38166; Grant number: PHSNS34492 (R.L.A., P.J.D.); Grant sponsor: Veterans Affairs Merit Review Grant (R.L.A.).

Drs. Tallaksen-Greene and Ordway contributed equally to this work.

*Correspondence to: Roger L. Albin, Room 4412D, Kresge III Building, 200 Zina Pitcher Place, Ann Arbor, MI 48109-0585.
E-mail: ralbin@umich.edu

Received 7 March 2003; Revised 30 April 2003; Accepted 8 May 2003
DOI 10.1002/cne.10855
Published online the week of August 25, 2003 in Wiley InterScience (www.interscience.wiley.com).

Nine human neurodegenerative diseases are caused by expanded CAG-polyglutamine (polyQ) repeats within nine unrelated genes. Huntington disease (HD; Huntington's Disease Collaborative Research Group, 1993), dentatorubropallidal-luysian atrophy (DRPLA), spinobulbar muscular atrophy (SMBA; Kennedy-Alter-Sung syndrome), and spinocerebellar ataxias 1, 2, 3 (synonymous with Machado-Joseph disease [MJD]), 6, 7, and 17 comprise the identified polyQ family of diseases (Taylor et al., 2002). Other than the CAG repeat sequences, these loci exhibit little sequence similarity. The expanded polyQ repeats may cause neurodegeneration by means of "gain of function" mechanisms by imparting novel neurotoxic properties. There are suggestions also of possible "loss of function" effects (Ferrer et al., 2000; Dragatsis et al., 2000; Zuccato et al., 2001). Common features of this disease family include dominant inheritance, anticipation of age of onset, length thresholds for the development of pathology around 38–40 CAG repeats (except for SCA6; [Jen, 2003]), and with the exception of SBMA, where dorsal root ganglia are affected, degeneration restricted to the central nervous system. Each polyglutamine repeat disorder has a unique regional pattern of neuropathology. Within affected regions, there is often subpopulation-specific loss of neurons (Iizuka and Hirayama, 1986; Gouw et al., 1994, Takiyama et al., 1994; Robitaille et al., 1995; Holmberg et al., 1998; Yang et al., 2000; Fujigasaki et al., 2001; Bazzett and Albin, 2001; Pulst, 2003).

Polyglutamine repeat diseases share a common histopathologic hallmark; intraneuronal aggregates of proteolytic fragments of the pathogenic protein containing the polyQ domain (Davies et al., 1997; Paulson et al., 1997; Becher et al., 1998). The inclusions are often ubiquinated and contain other proteins. Aggregates occur within the nucleus (neuronal intranuclear inclusions, NIIs) and the cytoplasm. There is good evidence that intranuclear localization of polyQ-containing fragments is a key step in the pathogenesis of neurodegeneration, but the specific pathogenic role of NIIs is unclear (Klement et al., 1998; Saudou et al., 1998; Kim et al., 1999; Cummings et al., 1999).

Ultrastructural evidence of NIIs in HD was published approximately 30 years ago, but their significance was unappreciated until their rediscovery in murine genetic models of HD (Tellez-Nagel et al., 1974; Mangiarini et al., 1996; Davies et al., 1997). The rediscovery of NIIs emphasizes the importance of murine genetic models. Transgenic and knockin murine models of several CAG repeat disorders have been created that reproduce several aspects of the human diseases (Burright et al., 1995; Ikeda et al., 1996; Mangiarini et al., 1996; Reddy et al., 1998; Hodgson et al., 1999; Levine et al., 1999; Sato et al., 1999; Schilling et al., 1999; Shelbourne et al., 1999; Huynh et al., 2000; Wheeler et al., 2000; La Spada et al., 2001; Lin et al., 2001; Katsuno et al., 2002; Watase et al., 2002; Yoo et al., 2003).

The common features of these diseases suggest common mechanisms of pathology driven by the expanded CAG repeats, modified possibly by expression patterns and surrounding sequences of the affected proteins. This inference predicts that expanded CAG repeats would be neurotoxic in any appropriately expressed "carrier" gene. We evaluated this prediction by developing a mouse line with 146 CAG repeats in the hypoxanthine phosphoribosyl transferase locus, ($Hprt^{(CAG)146}$), a gene that does not normally include CAG repeats. This line has adult-onset neurologic abnormalities, shortened life span, and widespread expression of NIIs, confirming the primary importance of the expanded CAG repeat domains (Ordway et al., 1997). Hprt is inactivated in these animals. Because Hprt inactivation in mice is devoid largely of major consequences, these results are consistent with the gain of function concept (Jinnah et al., 1991, 1992, 1994).

We report additional data on this line, including more precise determination of the age of onset of the behavioral changes, the time course of development of NIIs in mice characterized for behavioral abnormalities, the pattern of alterations in neurotransmitter markers, the integrity of mitochondrial electron transport chain markers, and susceptibility to the mitochodrial toxin 1-methyl-4-phenyl-1,2,3,6-tetrahydropyridine (MPTP).

MATERIALS AND METHODS

Mice

The $Hprt^{(CAG)146}$ knockin mouse line generated by gene targeting in mouse embryonic stem (ES) cells (Ordway et al., 1997) was used in all experiments. These studies were carried out on hemizygous males and homozygous females derived from breeding of heterozygous females with hemizygous males. *Hprt* is an X-linked locus and females express one copy of the locus due to X-inactivation. Offspring from these matings were genotyped by polymerase chain reaction using primers flanking the repeat region as described previously (Ordway et al., 1997). Initial work indicated no significant differences in the pathology of male and female mutants. Control animals were similarly gene-targeted mice with 70 CAG repeats inserted in the Hprt locus ($Hprt^{(CAG)70}$). These mice do not develop behavioral changes or NIIs and have normal life spans (Ordway et al., 1999).

Behavioral analysis

Twenty seven $Hprt^{(CAG)146}$ mice, 15 to 24 weeks old, were analyzed to more precisely define the age of onset of behavioral abnormalities. Animals younger than 15 weeks never showed behavioral abnormalities. Control animals were 12 $Hprt^{(CAG)70}$ mice, aged 24 to 64 weeks. Animals were housed separately for behavioral analysis. Cages were placed in a brightly lit laminar flow hood and cage tops removed. Normal mice will actively move about the cage under these conditions. Each mouse was scored as active if it roamed from its initial position or reared within 30 seconds of cage lid removal. Mice were then held suspended by the tail for 1 minute. Normal mice flail, extend limbs, and attempt to escape by climbing onto the tester's finger. Clasping of the fore- or hindlimbs is abnormal and was scored as present or absent. Mice able to climb onto the tester's finger within 1 minute were scored as escaping; those unable to escape were scored as abnormal. For rotarod analysis, mice were placed on a 4 cm diameter rotarod turning at 2.5 rpm 30 cm above a padded cage bottom (Ugo Basile, Comeria, Italy). Mice were scored as falling or not falling within a 60-second trial. Animals underwent 10 trials on 10 consecutive days. If a test was abnormal on 20% of trials, that animal was scored as abnormal on that test. If a seizure was witnessed during any trials, that animal was scored as having epilepsy. Animals were assigned a point for each abnormality on each test—diminished spontaneous activity, clasping, in-

ability to escape from suspension, falling from the rotarod within 60 sec, and presence of epilepsy—for a cumulative behavioral abnormality score with a possible total of 5 points. The higher the score, the greater number of behavioral abnormalities. Statistical analysis was performed between group behavioral abnormality scores with the nonparametric Mann–Whitney *U* test using the VassarStats program (http://faculty.vassar.edu/lowry/VassarStats.html).

Immunohistochemistry and quantification of NIIs

Mice were deeply anesthetized by intraperitoneal injection of Avertin (Aldrich, 0.4 mg/g i.p.) and perfused through the heart with approximately 100 ml of 0.1 M phosphate buffer (PB, pH 7.4) followed by approximately 100 ml of 4% paraformaldehyde in PB. Organs were removed, post-fixed overnight in 4% paraformaldehyde in PB and cryoprotected in sucrose/PB (up to 20% sucrose). Frozen brains were cut into 40-μm sections in the horizontal plane. Sections were sequentially collected in 1 in 5 series so that each group contained one section every 200 μm throughout the brain. Heart, liver, lung, kidney, spleen, testes, and skeletal muscle were processed similarly. Tissue sections were stained with rabbit polyclonal antiserum against ubiquitin (1:250 or 1:1,000 dilution; Dako) overnight at 4°C. Hprt immunoreactivity was visualized with a rabbit polyclonal antipeptide antisera directed against amino acids 7-17 of Hprt. The antiserum identified a single appropriate band on Western blots. For immunohistochemistry, both 1:500 and 1:2,000 dilutions were used and gave identical results. Primary antisera were diluted in PB, 0.3% Triton X-100, and 1.5% blocking serum. Processing was completed with the ABC method using Vectastain Elite kits (Vector Laboratories, Temecula, CA). Detection was performed by using a diaminobenzidine (DAB) substrate and $NiCl_2$ according to the manufacturer's recommended protocol (Vector Laboratories). Sections were dehydrated in graded alcohols and xylenes and mounted on gelatin-coated slides, and coverslips were affixed with Permount (Fisher, Pittsburgh, PA). Sections were viewed on a Nikon Eclipse E800 microscope. Adjacent series of sections were stained with 0.5% cresyl violet.

For quantification, ubiquitin-immunostained sections were used. By approximately 30 weeks of age, NIIs were found in virtually all regions examined. Regions were selected for quantification on the basis of relevance to human pathology (striatum, cerebellar cortex), early occurrence of NIIs (parabrachial nucleus), late occurrence of NIIs (globus pallidus), and to provide a representative sampling of other regions (frontal cortex, hippocampal formation, superior colliculus). NIIs were visualized by light microscopy at 800× and counted by using an ocular grid. To provide approximate frequencies of NIIs, the number of NIIs counted was divided by the number of cresyl violet–stained neurons in fields from the same areas of adjacent cresyl violet–stained sections. Cresyl violet–stained neurons were distinguished from glia by characteristic nuclear and nucleolar morphology. At least five fields were counted per brain region per brain. Brains were scored as lacking NIIs only after thoroughly scanning all sections within a group that included sections at 200-μm intervals throughout the brain. Parallel confirmatory experiments were performed with an N-terminal Hprt antiserum.

Receptor autoradiography

Hprt$^{(CAG)146}$ and control mice of various ages were killed by decapitation, and brains were extracted from the cranial vault, coated with Shandon–Lipshaw embedding matrix, and frozen in isopentane cooled by liquid N_2. Brains were stored at −70°C until time of sectioning. Brains were warmed to −20°C, and 12-μ sections were cut on a cryostat and thaw-mounted onto gelatin-coated slides and stored at −70°C.

Receptor autoradiography was performed as described previously (Richfield et al., 1989; Higgins and Greenamyre, 1996; Suzuki et al., 2001). To label type 2 vesicular monoamine transporter (VMAT2) binding sites, slides were prewashed for 5 minutes at room temperature (RT) in KBS-ethylenediaminetetraacetic acid buffer (pH 8.0), then incubated with 10 nM [^{3}H]methoxytetrabenazine (specific activity 82 Ci/mmol). Tetrabenazine (10 μM) was added to the ligand buffer to determine nonspecific binding. After incubation, sections were rinsed twice for 2 minutes in cold assay buffer, dipped in cold distilled water, and dried under cool air.

Assays for D1 and D2 dopamine receptors used a 25 mM Tris buffer (pH 7.2) with 100 mM NaCl, 1 mM $MgCl_2$, 1 μM pargyline and 0.001% ascorbic acid. For D1 receptors, slides were incubated with 0.55 nM [^{3}H]SCH23390 (specific activity 89 Ci/mmol) for 2.5 hours. Nonspecific binding was determined in the presence of 1 μM cis-flupentixol. For D2 receptors, slides were incubated in 0.75 nM [^{3}H]spiperone (specific activity 96 Ci/mmol) with 100 nM mianserin for 2.5 hours. Nonspecific binding was defined in the presence of 50 μM dopamine. After incubation, slides were rinsed in cold incubation buffer for 10 minutes, dipped in distilled water, and dried under cool air. Slides for γ-aminobutyric acid (GABA)/benzodiazepine receptor assays were prewashed for 30 minutes in cold assay buffer (50 mM Tris-citrate buffer, pH 7.2), air-dried, and incubated with 5 nM [^{3}H]flunitrazepam (specific activity 85 Ci/mmol) for 30 minutes at 4°C. Nonspecific binding was determined in the presence of 2 μM clonazepam in the ligand buffer. Sections were rinsed twice for 5 minutes in cold buffer and dried under warm air. Binding to complex I of the electron transport chain was examined by using 5 nM [^{3}H]dihydroxyrotenone (DHR; specific activity 60 Ci/mmol) in 50 mM Tris-HCl buffer, 1% bovine serum albumin (pH 7.6). Sections were incubated in ligand buffer for 2 hours at RT. Nonspecific binding was assessed by using 10 μM rotenone. Slides were rinsed in RT incubation buffer for 1 hour, followed by two 5-minute washes in 25 mM Tris-HCl (pH 7.6) and 15 seconds in distilled water, then dried under a stream of warm air.

Tritium-labeled slides were apposed to tritium-sensitive film (Hyperfilm ^{3}H or BioMax, Amersham) with calibrated radioactive standards and exposed for 2 to 5 weeks. Films were developed and analyzed by using a computer-based image analysis system (MCID, Imaging Research, St. Catharine's, Ontario, Canada). Image density corresponding to binding of tritiated ligand was converted to pmol/mg protein using the calibrated standards. Specific binding was determined by subtracting nonspecific from total binding. Results were analyzed by using the VassarStats program with a correlated *t* test.

Histochemistry

For cytochrome oxidase histochemistry, slides were incubated in 0.1 M HEPES buffer (pH 7.4) with 3.165 mM nickel ammonium sulfate, 117 mM sucrose, 16.15 μM cytochrome C, and 2.778 mM DAB for 30–45 minutes at 37°C. The sections were rinsed twice, 10 minutes each, in fresh HEPES buffer, dipped in distilled water, air-dried, dehydrated, and cover-slipped. For succinate dehydrogenase histochemistry, slides were incubated in 60 mM phosphate buffer (pH 7.0) with 0.04% nitro blue tetrazolium and 50 mM succinate for 45 minutes at 37°C. The sections were then soaked for 10 minutes in 4% paraformaldehyde in 50 mM Phosphate buffer (pH 7.0), rinsed in distilled water, dehydrated, and cover-slipped. Sections were analyzed by measuring optical density using a computer assisted MCID image analysis system (Imaging Research). Regional optical density was quantified using a uniform gray scale under uniform illumination conditions. Results were compared using a correlated *t* test with the VassarStats program.

MPTP lesions

Mice of varying ages and genotype were treated with 0, 20, or 40 mg/kg MPTP injected intraperitoneally in four divided doses given at 2-hour intervals. After 7 days, the animals were killed by decapitation. Groups included both male and female mice. Genders of mice were balanced within almost all groups, and there was no effect of gender on results. The forebrains were frozen and processed for autoradiography as described above.

Image preparation

Photomicrographs were prepared by photographing images with an Olympus BX-51 microscope equipped with SPOT-RT digital camera (Diagnostic Instruments, Sterling Heights, MI). Autoradiographic and histochemical images were captured with an MCID apparatus (Imaging Research). Images were imported into Photoshop 5.5 (Adobe, San Jose, CA) for adjustment of contrast, brightness, and sharpness.

RESULTS

Behavioral results

$Hprt^{(CAG)146}$ mice began to manifest significant behavioral changes at approximately 22 weeks of age. To confirm this impression, $Hprt^{(CAG)146}$ mice were divided into two groups; 15 to 21 weeks old (n = 15) and 22 to 24 weeks old (n = 11), and intergroup differences in cumulative behavioral abnormality scores (summation of all individual behavioral tests scored as normal or abnormal; see Materials and Methods section above) assessed with the nonparametric Mann–Whitney *U* test (Fig. 1). For the 15- to 21-week group, the mean rank was 8.7. For the 22- to 24-month group, mean rank was 20. This difference is significant ($P < 0.0002$; two-tailed test). The 22- to 24-week group was compared also with a group of $Hprt^{(CAG)70}$ control mice; 23 to 24 weeks old (n = 6), 26 to 29 weeks old (n = 2), and 60 to 64 weeks old (n = 4); total n = 12. The mean rank of $Hprt^{(CAG)70}$ mice was 6.7. The mean rank of the $Hprt^{(CAG)146}$ mice was 17.8. This difference is significant ($P < 0.0001$, two-tailed test). The $Hprt^{(CAG)146}$ mice 15 to 21 weeks old and the $Hprt^{(CAG)70}$ mice did not differ significantly in cumulative behavioral scores; both with mean rank of 14 ($P = 0.984$, two-tailed test). The normal results in $Hprt^{(CAG)70}$ mice and $Hprt^{(CAG)146}$ mice 15 to 21 weeks old are consistent with our prior experience with wild-type and Hprt knockout mice, where behavioral abnormalities on this battery of tests are seen only rarely, even in older animals (Ordway et al., 1997, 1999).

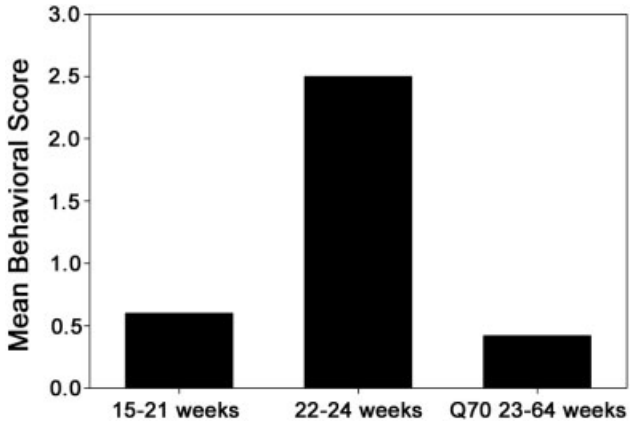

Fig. 1. Mean behavioral scores for $Hprt^{(CAG)146}$ mice, 15–21 weeks old, compared with $Hprt^{(CAG)146}$, 22–24 weeks old, and $Hprt^{(CAG)70}$ control mice. The 22- to 24-week age group has higher mean behavioral scores than younger or control mice.

Time course of occurrence of NIIs

NII occurrence was surveyed with ubiquitin immunohistochemistry in $Hprt^{(CAG)146}$ mice 15 to 18 weeks old, 20 to 26 weeks old, 32 to 38 weeks old, and 40 to 46 weeks old (n = 3–4 for each group). Assessing NII occurrence in older animals is difficult because of steeply rising mortality after 40 weeks. NII burden was assessed by estimating the percentage of Nissl-stained neurons expressing NIIs. No ubiquitin immunoreactive NIIs were found in the 15- to 18-week age group (Table 1; Fig. 2). In older animals, NIIs were detectable in varying numbers in all regions surveyed. In the 20- to 26-month age group, NIIs were present in a substantial percentage of neurons in the parabrachial nucleus and frontal cortex, i.e., 58% and 37%, respectively. Moderate percentages of NIIs (<20% and >10%) were present in cerebellar Purkinje cells, substantia nigra pars compacta neurons, superior colliculus neurons, and inferior colliculus neurons. Less than 10% of neurons in the hippocampal formation, striatum, globus pallidus, or substantia nigra pars reticulata expressed NIIs. In the 32- to 38-week age group, the regional distribution and percentage of NIIs was similar to that found in the 20- to 26-week age group with the possible exception of parabrachial neurons where the percentage of NII-containing neurons rose to 72%. In the 40- to 46-week age group, all regions exhibited abundant NIIs. Percentage of NIIs rose to 85% in the parabrachial nucleus and exceeded 60% in the frontal cortex, substantia nigra pars compacta, cerebellar Purkinje cells, and hippocampal formation. Percentage of NIIs exceeded 50% in striatal neurons, superior collicular neurons, and inferior collicular neurons. Even in regions with the lowest percentages of NIIs, the substantia nigra pars reticulata and the globus pallidus, percentage of neurons expressing NIIs was substantial, approximating 30%. Many regions displayed marked increases in

TABLE 1. NII Distribution as a Function of Age[1]

Animal age (week)	PN (%)	CTX (%)	PRK (%)	SNc (%)	SC (%)	IC (%)	HIP (%)	SNr (%)	STR (%)	GP (%)
15–18	0.0	0.0	0.0	0.0	0.0	0.0	0.0	0.0	0.0	0.0
20–26	57.8	36.6	18.0	17.1	16.4	16.3	7.5	4.7	4.5	3.8
32–38	72.0	22.7	23.3	20.9	11.7	7.5	10.0	7.8	4.8	7.2
40–46	84.6	63.4	64.9	65.6	50.5	58.7	65.9	31.9	56.6	27.5

[1]NIIs were identified with ubiquitin immunohistochemistry. Neurons were counted in parabrachial nuclei (PN), frontal cortex (CTX), cerebellar Purkinje cells (PRK), substantia nigra pars compacta (SNc), superior colliculus (SC), inferior colliculus (IC), hippocampus (HIP) substantia nigra pars reticulata (SNr), striatum (STR), and globus pallidus (GP). NII-positive neurons were counted manually using an eyepiece graticule in randomly selected fields. Total Nissl-stained neurons were counted in the same fields, and results are expressed as percentage of total neurons per field. N = 3–4 per group.

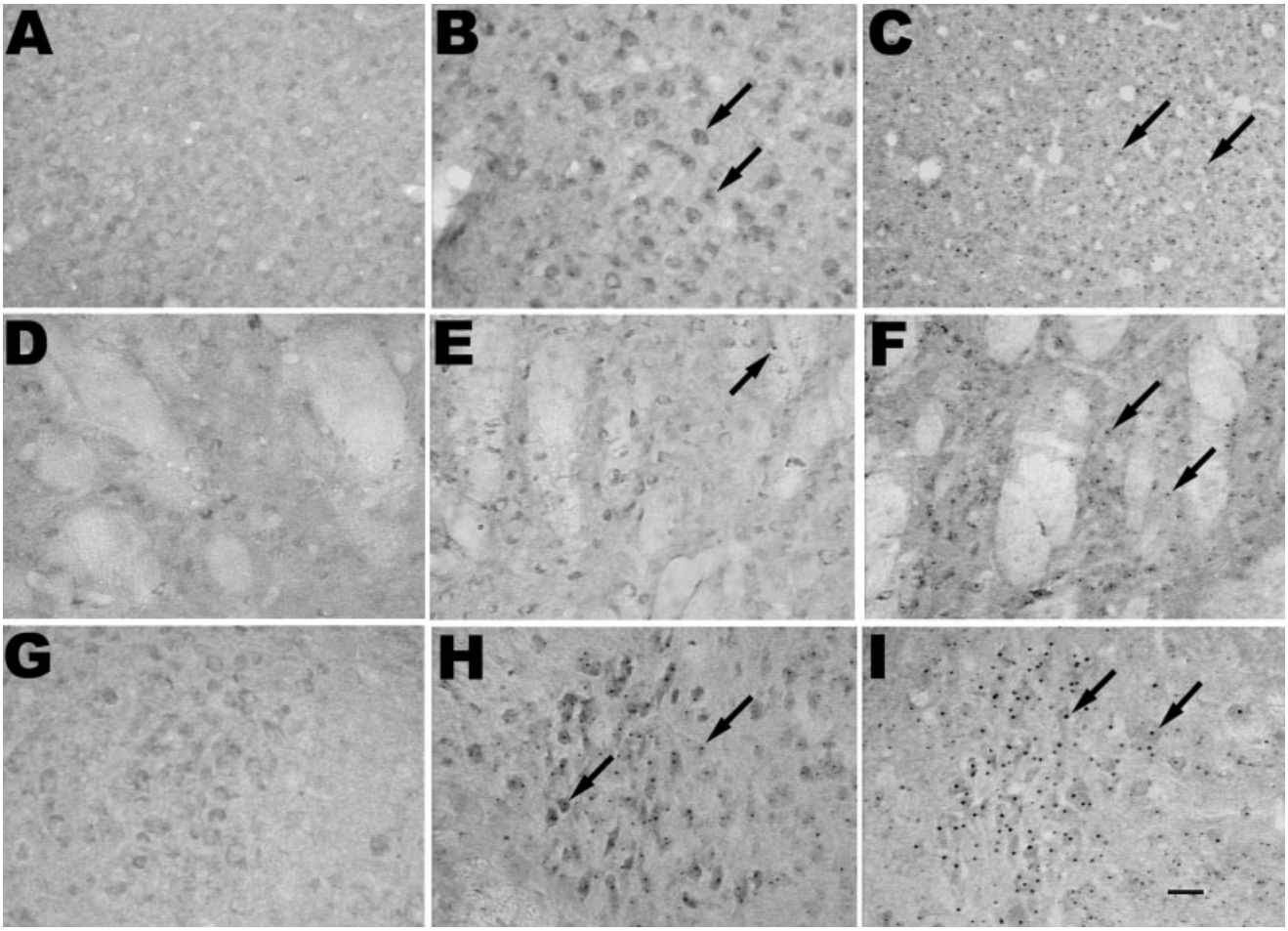

Fig. 2. Ubiquitin-immunoreactive neuronal intranuclear inclusions. Regions are cerebral cortex (**A–C**), striatum (**D–F**), and parabrachial nucleus (**G–I**) at 15 weeks (A,D,G), 26 weeks (B,E,H), and 40 weeks (C,F,I). Arrows mark representative inclusions. Scale bar = 75 μm in I (applies to A–I).

the percentage of neurons containing NIIs in the interval between the 32- to 38-week and 40- to46-week age groups. In the frontal cortex, cerebellar Purkinje cells, globus pallidus and substantia nigra pars compacta, there was a two- to threefold increase the percentage of neurons containing NIIs. In the remaining regions, the magnitude of the increase was greater, approximately 5- to 10-fold. Similar results were found with anti-Hprt antisera (Fig. 3).

NIIs in non–central nervous system tissue

Non–central nervous system tissues were studied in two mutants, 30 and 46 weeks of age, and two wild-type mice. NIIs were found in hepatocytes but not in heart, lung, kidney, spleen, testes, or muscle (Fig. 4). NIIs were seen also in choroid plexus epithelium (Fig. 4).

Receptor binding studies

GABA/benzodiazepine receptor, D1-like receptor, D2-like receptor, and VMAT2 binding sites were assessed before and after the onset of behavioral abnormalities in Hprt$^{(CAG)146}$ mice. Animals were assessed at approximately 16 weeks (n = 4) and 45 weeks of age (n = 7). These results were compared with results from older (approximately 55 week) Hprt$^{(CAG)70}$ mice as described in the

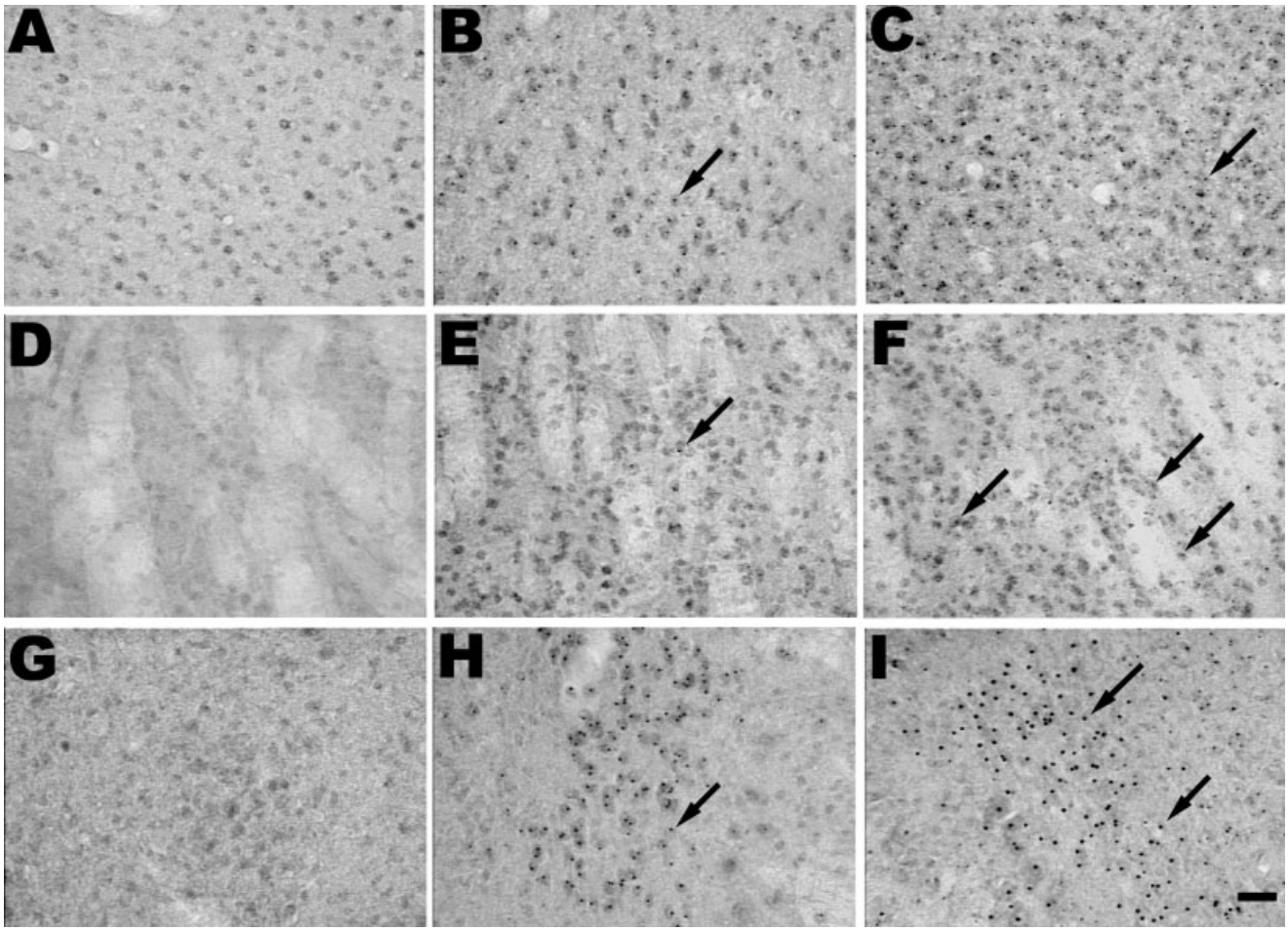

Fig. 3. Hprt-immunoreactive neuronal intranuclear inclusions. Regions are cerebral cortex (**A–C**), striatum (**D–F**), and parabrachial nucleus (**G–I**) at 15 weeks (A,D,G), 26 weeks (B,E,H), and 40 weeks (C,F,I). Arrows mark representative inclusions. Scale bar = 75 μm in I (applies to A–I).

Material and Methods section. Additional controls included younger (16 week; n = 4), middle aged (30 week; n = 4), and older (51 week; n = 4) wild-type mice with intact Hprt and older $Hprt^{(CAG)39}$ mice (51 week; n = 2). Results from these controls were virtually identical to results obtained from $Hprt^{(CAG)70}$ mice (data not shown), and $Hprt^{(CAG)70}$ mice are believed to be the best control group for $Hprt^{(CAG)146}$ mice. At 16 weeks and 45 weeks, there were not changes in GABA/BDZ binding sites in any region (Table 2; Fig. 5). D1-like receptor and D2-like receptor binding sites were significantly reduced in the striatal complex (striatum proper, nucleus accumbens, olfactory tubercle) of older (45 week) but not younger (16 week) $Hprt^{(CAG)146}$ mice (Table 3; Fig. 5). In the substantia nigra, D1-like receptor binding sites were reduced similarly in older $Hprt^{(CAG)146}$ mice. In the nigra, the great majority of D1-like receptor binding sites are on striatonigral terminals, and this finding is likely to reflect either reduced synthesis of D1-like receptors by striatal projection neurons or loss of striatal terminals within the substantia nigra. There was a trend toward increased substantia nigra D2-like receptor binding. Nigral D2-like receptors are expressed by substantia nigra dopaminergic neurons, and this increase could represent a concentrative effect of loss of surrounding neuropil due to degeneration of afferent striatal projection neuron terminals. VMAT2 binding, a measure of striatal dopaminergic terminals, was markedly reduced in the striatal complex and substantia nigra of older $Hprt^{(CAG)146}$ mice (Table 3; Fig. 5). In the younger $Hprt^{(CAG)146}$ mice, VMAT2 binding was reduced in the striatum proper, and there was a trend toward reduced VMAT2 binding in the nucleus accumbens, olfactory tubercle, and substantia nigra. Alterations in VMAT2 binding were the only changes we detected before the onset of behavioral changes or NII formation. Striatal VMAT2 binding is usually interpreted as a function of striatal dopamine terminal integrity but altered expression of VMAT2 is another possible explanation for this finding.

Mitochondrial electron transport chain activities

Complex I expression was assessed with [^{3}H]DHR binding, whereas Complex II/III and Complex IV activities

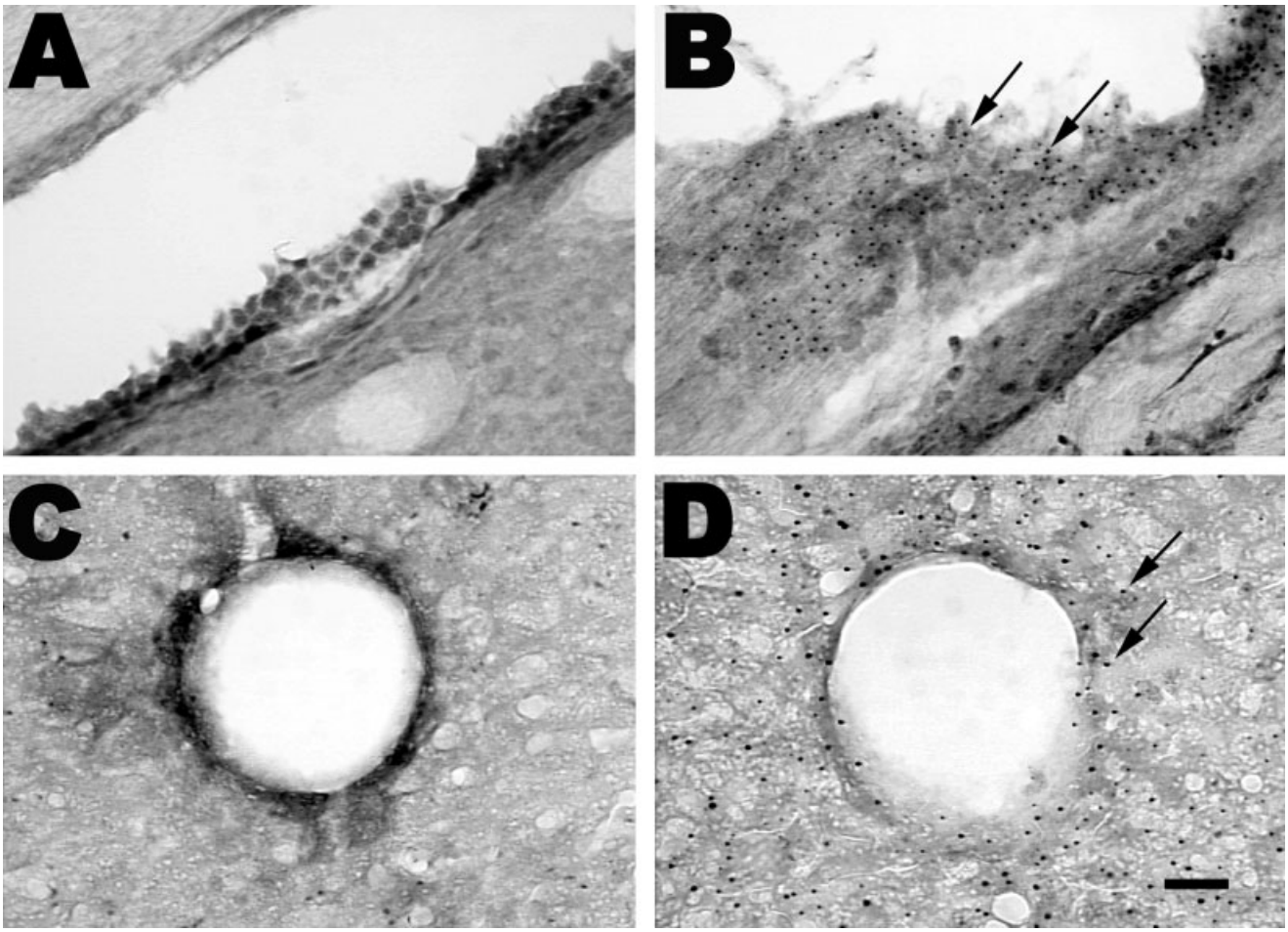

Fig. 4. Neuronal intranuclear inclusions in non–central nervous system tissues. Ubiquitin-immunoreactivity in choroid plexus epithelium and liver of 30-week-old wild-type mouse (**A,C**) and 46-week-old Hprt$^{(CAG)146}$ mouse (**B,D**). Arrows mark representative inclusions. Scale bar = 75 μm in D (applies to A–D).

TABLE 2. [^{3}H]Flunitrazepam Binding[1]

Genotype	*n*	Age in weeks (±SEM)	Striatum	nAccumbens	SNc	TempCx	FrPar Cx	Hippo	MlCblm	GclCblm
HprtQ146	7	44.94 (1.0)	102.57 (18.46)	123.01 (10.22)	90.50 (9.34)	119.21 (5.16)	105.12 (5.42)	99.20 (11.49)	101.85 (16.54)	130.15 (35.35)
HprtQ146	4	16.5 (0.5)	94.48 (13.92)	108.88 (11.19)	95.18 (6.73)	98.11 (4.37)	83.50 (6.73)	91.55 (8.86)	95.65 (10.46)	112.98 (17.75)
HprtQ70	7	55.0 (1.5)	100.00	100.00	100.00	100.00	100.00	100.00	100.00	100.00

[1]nAccumbens, nucleus accumbens; SNc, substantia nigra, pars compacta; TempCx, temporal cortex; FrPar Cx, frontoparietal cortex; Hippo, hippocampus; MlCblm, molecular layer of the cerebellar cortex; GclCblm, granular cell layer of the cerebellar cortex. Data are percentage of regional specific binding of [^{3}H]flunitrazepam (± SEM) relative to [^{3}H]flunitrazepam specific binding in aged Q70 animals. Specific binding determined by receptor autoradiography with conversion of film optical density to bound radioactivity using coexposed radioactive standards to generate a standard curve relating optical density to radioactivity. None of the comparisons reached significance at $P < 0.05$.

were assessed histochemically with succinate dehydrogenase (SDH) and cytochrome oxidase (CyOx) histochemistry, respectively. [^{3}H]DHR binding was measured in young (16 week; n = 4) and older (45 week; n = 7) Hprt$^{(CAG)146}$ mice. Controls were older (56 week; n = 12) Hprt$^{(CAG)70}$ mice. In all regions evaluated of older Hprt$^{(CAG)146}$ mice, there was a nonsignificant trend toward increases in [^{3}H]DHR binding compared with Hprt$^{(CAG)70}$ mice (Table 4; Fig. 6). Younger Hprt$^{(CAG)146}$ mice were indistinguishable from Hprt$^{(CAG)70}$ mice. Similar results were obtained with SDH and CyOx histochemistry (Table 4; Fig. 6). In all brain regions examined in all age groups, there was no difference in SDH or CyOx activity between Hprt$^{(CAG)146}$ and Hprt$^{(CAG)70}$ mice.

Susceptibility to MPTP

To assess the vulnerability of Hprt$^{(CAG)146}$ mice to mitochondrial impairment, we chose the neurotoxin MPTP. MPTP is a protoxin selective for dopaminergic neurons. MPTP is converted to MPP^+ with the latter species selectively accumulated in dopaminergic neurons where it inhibits Complex I. We chose this approach because of ease

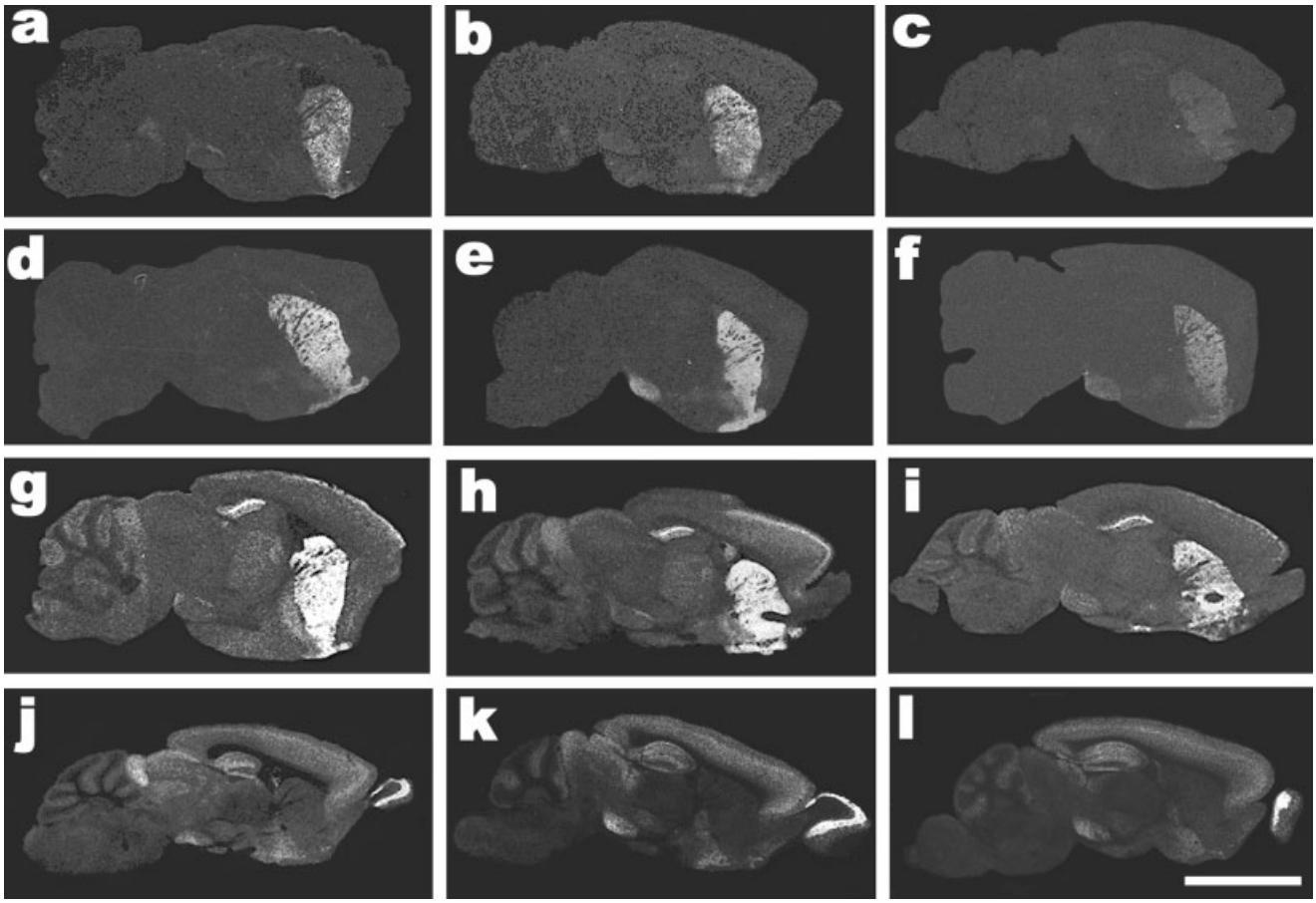

Fig. 5. Autoradiographs of type 2 vesicular monoamine transporter (VMAT2) expression (**a–c**), D1 receptor expression (**d–f**), D2 receptor expression (**g–i**), and benzodiazepine/GABA-A receptor expression (**j–l**). Columns are 16-week-old Hprt$^{(CAG)146}$ mice (a,d,g,j), 55-week-old Hprt$^{(CAG)70}$ control mice (b,e,h,k), and 45-week-old Hprt$^{(CAG)146}$ mice (c,f,i,l). Striatal VMAT2 expression is reduced in both young and older Hprt$^{(CAG)146}$ mice. Striatal D1 receptor and D2 receptor expression are reduced in older Hprt$^{(CAG)146}$ only. Benzodiazepine/GABA-A receptor expression is unchanged in young and old Hprt$^{(CAG)146}$. Scale bar = 5 mm in i (applies to a–i).

TABLE 3. Striatal–Nigral Dopamine Receptors and Terminals[1]

Genotype	*n*	Age in weeks (±SEM)	Striatum	nAccumbens	OT	SN
D1 receptors						
HprtQ146	7	44.9 (1.0)	**63.05** (6.16)	**66.90** (4.43)	**52.80** (4.82)	**73.93** (8.00)
HprtQ146	4	16.5 (0.5)	96.40 (8.07)	91.11 (14.61)	82.56 (13.48)	77.94 (9.97)
HprtQ70	8	55.1 (1.28)	100.00	100.00	100.00	100.00
D2 receptors						
HprtQ146	7	44.9 (1.0)	**52.00** (4.56)	**61.16** (4.87)	**61.03** (5.77)	**178.02** (64.19)
HprtQ146	4	16.5 (0.5)	94.65 (4.05)	95.718 (7.12)	81.47 (8.43)	85.78 (28.79)
HprtQ70	7	54.6 (1.3)	100.00	100.00	100.00	100.00
Dopamine terminals						
HprtQ146	7	44.9 (1.0)	**30.92** (8.01)	**37.81** (8.12)	**38.83** (8.63)	**58.11** (11.56)
HprtQ146	4	16.5 (0.5)	**57.38** (7.11)	75.61 (8.68)	84.82 (6.75)	77.84 (9.46)
HprtQ70	8	55.4 (1.3)	100.00	100.00	100.00	100.00

[1]nAccumbens, nucleus accumbens; OT, olfactory tubercule; SN, substantia nigra. Data are percentage of specific binding of [^{3}H]SCH23390 for D1 receptors, [^{3}H]spiperone for D2 receptors, [^{3}H]methoxytetrabenazine for dopamine terminals (± SEM) relative to specific ligand binding in aged Q70 animals. Specific binding determined by receptor autoradiography with conversion of film optical density to bound radioactivity using coexposed radioactive standards to generate a standard curve relating optical density to radioactivity. Bold values are significantly different from control values ($P < 0.05$).

of MPTP administration and ease of measurement of striatal dopamine terminal density with the VMAT2 ligand [^{3}H]MTBZ. Expression of NIIs within substantia nigra pars compacta neurons suggested that these neurons might be more vulnerable to mitochondrial impairment (Ordway et al., 1997). Hprt$^{(CAG)146}$ mice at varying ages (12–22 weeks, n = 3–5; 27–32 weeks, n = 5; 42–55 weeks, n = 5–6) were evaluated after receiving 0 mg/kg, 20 mg/kg, and 40 mg/kg of MPTP as described in the Materials and Methods section. The control animals were Hprt$^{(CAG)70}$ mice. As described above, there was a decline in VMAT2 binding in the vehicle-treated Hprt$^{(CAG)146}$

TABLE 4. Electron Transport Chain Measures[1]

Genotype	Age (weeks)	*n*	Region	DHR Binding	SDH	CyOx
HprtQ146	12–22	3–4	Striatum	103.46[2]	0.252	0.435
HprtQ146	12–22	3–4	Sensorimotor cortex	129.39[2]	0.235	0.530
HprtQ146	45	5–7	Striatum	134.81[2]	0.268	0.436
HprtQ146	45	5–7	Sensorimotor cortex	123.50[2]	0.263	0.610
HprtQ70	12–22	4–12	Striatum	100	0.321	0.423
HprtQ70	12–22	4–12	Sensorimotor cortex	100	0.281	0.529
HprtQ70	45	4–12	Striatum	100	0.287	0.444
HprtQ70	45	4–12	Sensorimotor cortex	100	0.257	0.549

[1]DHR, [^{3}H]dihydrotenone binding; SDH, succinate dehydrogenase activity; CyOx, cytochrome oxidase activity. DHR binding is expressed as percentage of specific [^{3}H]Dihydrotenone binding in HprtQ70 animals. SDH and CyOx activity measured as optical density of regions on fresh frozen cryostat prepared sections with standard histochemical methods (see Materials and Methods section for details). No difference found between young or aged HprtQ146 or HprtQ70 mice. Similar results found in other brain regions (data not shown) and also after regional optical density was normalized to whole brain optical density. Hprt, hypoxanthine phosphoribosyl transferase locus.
[2]DHR binding is specific binding of [^{3}H]dihydrotenone determined by receptor autoradiography with conversion of film optical density to bound radioactivity using coexposed radioactive standards to generate a standard curve relating optical density to radioactivity.

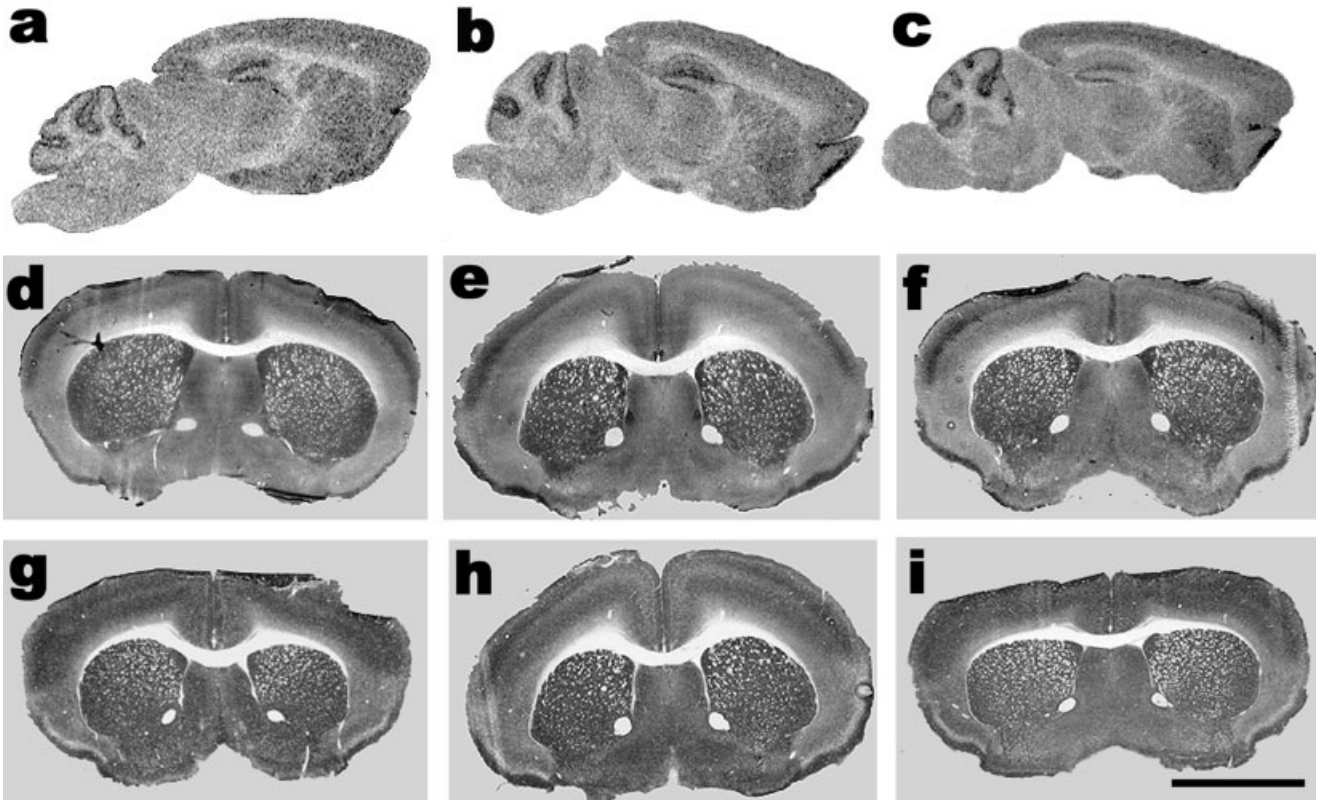

Fig. 6. Electron transport chain measures in young (16 weeks, **a,d,g**), aged (45 weeks, **c,f,i**) Hprt$^{(CAG)146}$, and aged (45 week, **b,e,h**) Hprt$^{(CAG)70}$ control mice. Top row (a–c) is [^{3}H]dihydrorotenone binding to complex I; second row (d–f) is succinate dehydrogenase activity, and third row (g–i) is cytochrome oxidase activity. There is no difference between young Hprt$^{(CAG)146}$ mice, aged Hprt$^{(CAG)146}$ mice, and aged control Hprt$^{(CAG)70}$ mice. Scale bar = 3 mm in i (applies to d–i); 4 mm in a–c.

mice compared with Hprt$^{(CAG)70}$ mice. In contrast to the results described above, differences between Hprt$^{(CAG)70}$ and Hprt$^{(CAG)146}$ mice were not seen in the youngest mice. This finding is probably because this experiment included some younger animals (12 weeks) than the experiments described above (16 weeks). A total of 40 mg/kg MPTP treatment reduced striatal VMAT2 binding sites in both Hprt$^{(CAG)146}$ and Hprt$^{(CAG)70}$ mice at young and older ages (Table 5; Fig. 7). The magnitude of the reduction in striatal VMAT2 binding, as measured by percentage loss of striatal VMAT2 binding compared with vehicle-treated controls was actually greater in Hprt$^{(CAG)70}$ mice than in Hprt$^{(CAG)146}$ mice (Table 5). In the oldest Hprt$^{(CAG)70}$ mice, the effect of MPTP appeared to be greater than in the youngest Hprt$^{(CAG)70}$ mice. Although the vehicle-treated controls had very similar levels of striatal VMAT2 binding, the percentage decline in striatal VMAT2 binding after 40 mg/kg treatment was approximately twice as great in the older animals. Similarly, although the 20 mg/kg dose produced no effect in younger Hprt$^{(CAG)70}$ mice, there was an effect in the oldest Hprt$^{(CAG)70}$ mice. There is no differential effect of MPTP between Hprt$^{(CAG)146}$ and Hprt$^{(CAG)70}$ mice, and there may be an age enhanced susceptibility to MPTP in Hprt$^{(CAG)70}$ mice.

DISCUSSION

Age of onset of behavioral abnormalities

We showed previously that Hprt$^{(CAG)146}$ mice develop adult-onset behavioral abnormalities, have premature mortality, and exhibit abundant NIIs (Ordway et al., 1997). Consistent with prior data, cumulative behavioral scores became abnormal at approximately 22 weeks of age. Repeat length is an important determinant of age of onset and penetrance (Stine et al., 1993; Rubinsztein et al., 1996). Over some threshold, repeat number correlates inversely with age of onset of clinical disease (Huntington's Disease Collaborative Research Group, 1993; Rubinsztein et al., 1997) and accounts for approximately 50% of the variance in age of onset. In murine genetic models, repeat number and the amount of gene product have influenced age of onset (reviewed in Zoghbi and Botas, 2002). In transgenic models, expanded CAG repeats in truncated constructs and/or high expression of transgenes are required to produce a phenotype. With knockin models of HD and SCA1, significant behavioral phenotypes develop only with CAG repeat expansions greater than those found typically in human patients (Lin et al., 2001; Menalled et al., 2002; Wheeler et al., 2002; Zoghbi and Botas, 2002; Watase et al., 2002). The relatively short life span of mice may limit the opportunity to observe the effects of repeat lengths that are pathogenic in humans. Existing methods of behavioral evaluation may also be insufficiently robust to detect earlier changes.

The amount of mutant protein produced may also affect age of onset. The R6 transgenic HD lines developed by Bates' group vary in repeat number and levels of protein expression (Mangiarini et al., 1996). Lines with higher repeat numbers and higher levels of protein expression have a more aggressive phenotype. In a transgenic yeast artificial chromosome (YAC) model of HD with 43 repeats, abnormalities are found only with supranormal expression levels of the mutant protein (Reddy et al., 1998). In our knockin model of HD, mutant homozygous animals develop behavioral abnormalities at an earlier age than heterozygous animals (Lin et al., 2001). Similar effects of homozygosity are found in a knockin model of SCA7 (Yoo et al., 2003). Homozygous HD mutation carriers were reported originally to have clinical disease indistinguishable from heterozygotes, but recent data indicates that HD homozygotes have a more aggressive clinical course than heterozygotes (Wexler et al., 1987; Squitieri et al., 2003). Earlier age of onset is reported in SCA3/MJD and DRPLA homozygotes (Sato et al., 1995; Sobue et al., 1996).

TABLE 5. Effects of MPTP on Dorsal Striatal [^{3}H]MTBZ Binding[1]

Group	Young *12–22 wk*	Mid *27–32 wk*	Old *42–55 wk*
Q146, Q146/146			
MPTP 0	100.2 (3)	60.8 (5)	73.1 (5)
MPTP 20	115.0 (3)	61.9 (5)	54.5 (5)
MPTP 40	66.5 (5)	34.1 (5)	40.6 (6)
Q70, Q70/70			
MPTP 0	96.7 (5)	74.4 (1)	100.0 (4)
MPTP 20	111.3 (5)	90.0 (1)	66.2 (5)
MPTP 40	78.8 (5)	33.5 (1)	41.9 (4)
Q39, Q39/39			
MPTP 0	97.3 (2)	90.7 (2)	155.8 (2)
MPTP 20	112.6 (2)	89.0 (2)	98.0 (2)
MPTP 40	86.1 (2)	42.0 (2)	56.5 (1)

[1]MPTP 0 = vehicle administered, MPTP 20 = 20 mg/kg MPTP, MPTP 40 = 40 mg/kg MPTP. [^{3}H]MTBZ binding to dorsal striatal dopamine terminals determined by receptor autoradiography with conversion of film optical density to bound radioactivity using coexposed radioactive standards to generate a standard curve relating optical density to radioactivity. Values expressed as percentage of striatal specific [^{3}H]MTBZ binding in *Q39* and *Q146* relative to specific [^{3}H]MTBZ binding in old *Q70* MPTP 0 animals. Numbers in parentheses after percent values are the number of each group. There is no difference in the effects of MPTP on [^{3}H]MTBZ binding between *Q146, Q70,* and *Q39* animals. MPTP, 1-methyl-4-phenyl-1,2,3,6-tetrahydropyridine.

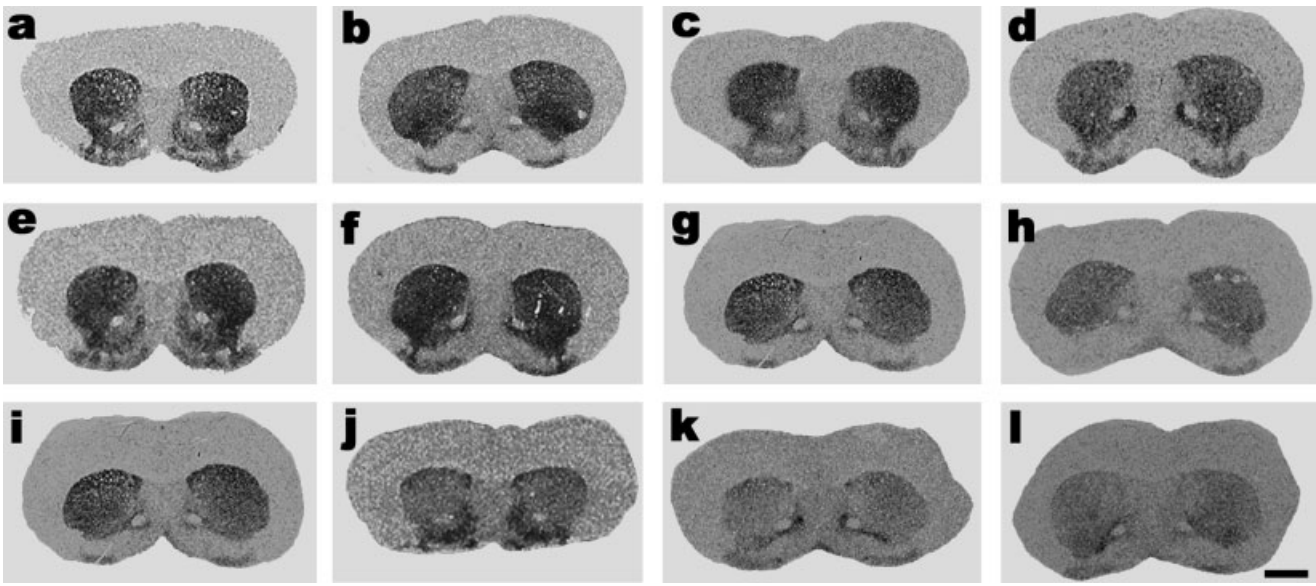

Fig. 7. Effects of 1-methyl-4-phenyl-1,2,3,6-tetrahydropyridine (MPTP) intoxication on Hprt$^{(CAG)146}$ and Hprt$^{(CAG)70}$ control mice of different ages. Amounts administered are 0 mg/kg MPTP(**a–d**), 20 mg/kg MPTP (**e–h**), 40 mg/kg (**i–l**). First column (a,e,i) is 13-week Hprt$^{(CAG)70}$ mouse, second column (b,f,j) is 16-week Hprt$^{(CAG)146}$ mouse, third column (c,g,k) is 45-week Hprt$^{(CAG)70}$ mouse, fourth column (d,h,l) is 45-week Hprt$^{(CAG)146}$ mouse. There is no difference in MPTP effects at any age or dose of MPTP. Scale bar = 1.5 mm in l (applies to a–l).

Time course of NII accumulation

The role of NIIs in neurodegeneration is controversial. By analogy with other forms of insoluble protein pathology, e.g., Lewy bodies and amyloid plaques, NIIs and cytoplasmic inclusions are suggested to be proximate causes of neurodegeneration in CAG repeat disorders (Davies et al., 1997; Ross, 1997, 2002; Scherzinger et al., 1997; Becher et al., 1998; Sisodia, 1998; Trojanowski and Lee, 2000). Alternative interpretations of the role of NIIs are that they are epiphenomena or that they could be protective (Ordway et al., 1997; Sisodia, 1998; Ross, 2002; Zoghbi and Botas, 2002).

NIIs were first visualized at approximately the same age as the development of behavioral abnormalities. In almost all regions studied, there was a marked increase in the percentage of neurons expressing NIIs in the 40 to 46 week age group, paralleling the ages at which mortality accelerates. This type of analysis cannot, however, establish causal relations between NIIs and behavioral abnormalities. We relied on ubiquitin immunohistochemistry to quantify the presence of NIIs. Aggregation of polyglutamine repeat-containing protein fragments may occur earlier than easily demonstrable ubiquination. In HD knockin mice, nuclear localization of *huntingtin* is an early event and emergence of *huntingtin*-immunoreactive NIIs precedes the development of ubiquitin-immunoreactive NIIs (Wheeler et al., 2000; Tallaksen-Greene et al., unpublished data). With anti-Hprt antisera, we found a similar time course for NII emergence but our reliance on ubiquitin immunohistochemistry for quantification may underestimate the age of occurrence of NIIs and the apparent correlation with behavioral abnormalities may be spurious.

We found one region where evidence of neuronal dysfunction is dissociated from NII occurrence, the substantia nigra pars compacta (SNpc). Dorsal striatal [^{3}H]MTBZ binding was decreased before NII occurrence in the SNpc. [^{3}H]MTBZ binding is an excellent marker of nigrostriatal dopaminergic afferents (Vander Borght et al., 1995a, b). Diminished [^{3}H]MTBZ binding is due to either loss of nigrostriatal dopaminergic afferents or relative down-regulation of VMAT2 expression. Decreased striatal [^{3}H]MTBZ binding is a likely marker of neuronal dysfunction. Dissociation of NII expression from [^{3}H]MTBZ binding changes argues against a primary pathogenic role for NIIs in neurodegeneration.

In vitro and in vivo experiments dissociated the toxic effects of expanded CAG repeat-containing intranuclear fragments from NII formation (Saudou et al., 1998; Klement et al., 1998; Kim et al., 1999; Cummings et al., 1999; Simeoni et al., 2000; Mastroberardino et al., 2002; Menalled et el., 2002; Watase et al., 2002). In HD, there is not a good correlation between striatal neuron subpopulation expression of NIIs and the pattern of striatal neuron subpopulation degeneration (DiFiglia et al., 1997; Kuemmerle et al., 1999). In SCA2, NIIs are expressed sparsely and without good correlation with the pattern of neurodegeneration (Huynh et al., 2000). NIIs are probably not key mediators of pathogenesis in polyglutamine repeat disorders. NIIs could play a protective role by acting as a "sink" for toxic expanded CAG repeat-containing proteolytic fragments, and neurons able to form NIIs may be relatively protected against the effects of expanded CAG repeats. Oligomerization of polyglutamine-containing fragments, however, may be a key step in pathogenesis. Disruption of oligomerization with the azo-dye Congo Red, extends life span and reduces NII burden in R6/2 mice (Sanchez et al., 2003). The role of NIIs could be multifactorial. In our data set, abundant NIIs were found in all regions examined around the period when mortality rates accelerated. NIIs may act as a protective sink in the early stages of neuronal injury but assume a pathogenic role later in the course of the disease.

Nuclear inclusions in non-neuronal tissues

We found nuclear inclusions in two non-neuronal cell populations: hepatocytes and choroid plexus epithelium. The relative lack of nuclear inclusions in non-neuronal cells is interesting in view of the widespread expression of Hprt. In R6/2 mice, which have diabetes, nuclear inclusions have been found in pancreatic islet cells, skeletal and cardiac muscle fibers, adrenal cortical cells, and myenteric plexus neurons (Hurlbert et al., 1999; Sathasivam et al., 1999). It is unknown why NIIs are expressed preferentially in neurons and why neurons are particularly susceptible to the toxic effects of polyglutamine expansions. Neurons are unusually long lived postmitotic cells with an essentially zero rate of turnover in almost all brain regions. Even low rates of cell turnover might purge cells accumulating toxic polyglutamine-containing fragments. Some mitotically active cell populations express NIIs in R6/2 mice, and we did find nuclear inclusions in hepatocytes, a renewable cell type. Factors governing the expression of NIIs are likely to be complex, possibly including cell-specific differences in cell life span and metabolism of expanded polyglutamine-containing proteins.

Neurotransmitter marker changes and transcriptional dysregulation

We found differential effects on neurotransmitter markers in Hprt$^{(CAG)146}$ mice. In both young and older Hprt$^{(CAG)146}$ mice, there was no effect on expression of GABA/benzodiazepine receptor binding sites. Striatal D1-like and D2-like receptor binding site expression was diminished in older animals. Dorsal striatal VMAT2 binding was diminished significantly before the development of behavioral abnormalities and the occurrence of NIIs. The normal expression of GABA/benzodiazepine receptor binding sites argues against nonspecific loss of neurotransmitter marker binding sites due to neurodegeneration or nonspecific neuronal dysfunction. A similar result was described in the R6/2 model of HD (Cha et al., 1998; Reynolds et al., 1999). Of interest, in this line, there is a similar decline in striatal dopamine terminal markers when markers of intrinsic striatal neurons are preserved (Reynolds et al., 1999; Hickey et al., 2002). A likely explanation for this pattern of findings is selective loss of specific neurotransmitter markers due to transcriptional dysregulation (Luthi-Carter et al., 2000).

Considerable evidence indicates that transcriptional dysregulation is not merely an epiphenomenon but central to the pathogenesis of neurodegenerative polyglutamine repeat disorders (Perutz et al., 1994; Boutell et al., 1999; Lin et al., 2000; Luthi-Carter et al., 2000; McCampbell et al., 2000, 2001; Holbert et al., 2001; Nucifora et al., 2001; Steffan et al., 2000, 2001; Chai et al., 2001, 2002; Zhang et al., 2002; Dunah et al., 2002; Katsuno et al., 2002; Takeyama et al., 2002; Kegel et al., 2002). Evidence from in vitro models and genetic models indicates that nuclear

localization of expanded polyglutamine-containing polypeptides, possibly in the form of caspase-produced fragments, is a crucial step in pathogenesis (Goldberg et al., 1996; Wellington et al., 1998, 2002; Li et al., 2000; Kim et al., 2001). For a dissenting view, however, see Dyer and McMurray (2001). Expanded polyglutamine-containing polypeptides may aggregate with and sequester proteins involved in transcription (Boutell et al., 1999; McCampbell et al., 2000, 2001; Holbert et al., 2001; Nucifora et al., 2001; Steffan et al., 2000; Chai et al., 2001, 2002; Zhang et al., 2002; Dunah et al., 2002; Kegel et al., 2002). Evidence from both human postmortem tissue and murine genetic models of HD, SCA1, and DRPLA indicates altered transcription in these diseases. Overexpression of sequestered transcriptionally active proteins reverses some of the effects of mutant *huntingtin* and *atrophin* in some model systems (Shimohata et al., 2000; Nucifora et al., 2001; Dunah et al., 2002).

Transcriptional dysregulation is a plausible mechanism for explaining the regional and subregional specificity of neurodegeneration characteristic of polyglutamine diseases. Different populations of neurons express different complements of proteins active in transcription. Differential affinity of these proteins for the different expanded polyglutamine-containing protein fragments could explain differential regional and subregional neurodegeneration. This model is supported by results from a murine transgenic model of SCA7 where specific interference with the homeobox protein CRX is suggested to underlie retinal degeneration (La Spada et al., 2001). On the other hand, recent data from a knockin model of SCA7 contradicts this result (Yoo et al., 2003).

Mitochondrial dysfunction

One creditable proximate cause of neurodegeneration in HD is excitotoxic injury. Acute N-methyl-D-aspartate (NMDA) receptor agonist striatal excitotoxic lesions are remarkable mimics of HD striatal pathology (Bazzett and Albin, 2001). The most popular version of the excitotoxic hypothesis suggests that mitochondrial dysfunction increases neuronal susceptibility to NMDA receptor-mediated excitotoxic injury, so-called indirect excitotoxicity. Compounds that inhibit electron transport chain activity cause striatal lesions with many features of HD striatal pathology (Beal et al., 1993a, b; Greene and Greenamyre, 1995; Bazzett et al., 1995). Several in vitro and in vivo studies describe mitochondrial dysfunction in HD or murine genetic models of HD (Jenkins et al., 1993; Browne et al., 1997; Sawa et al., 1999, Tabrizi et al., 2000; Panov et al., 2002). Guidetti et al. (2001), however, did not find evidence of mitochondrial dysfunction in early postmortem HD material. The excitotoxic hypothesis predicts that murine genetic models of HD should exhibit increased susceptibility to mitochondrial toxins and/or NMDA agonists. Conflicting data exist on this point (Bogdanov et al., 1998; Hansson et al., 1999, 2001a, b; Levine et al., 1999; Zeron et al., 2002). A large clinical trial based on the indirect excitotoxicity hypothesis evaluated coenzyme Q10 (ubiquinone) as a mitochondrial function booster and the NMDA receptor antagonist remacemide (Huntington Study Group, 2001). There was no significant effect of either compound or the combination, although positive effects were seen in the R6/2 mouse model (Ferrante et al., 2002).

Our data do not support the notion of mitochondrial dysfunction or increased susceptibility to mitochondrial toxins. The indirect excitotoxic hypothesis is plausible, but more evidence will be required to demonstrate its relevance to polyglutamine diseases.

Knockin vs. transgenic models

A theoretical advantage of this model and other "knockin" murine genetic models is that the expanded CAG repeat sequences are expressed in the context of their normal patterns of expression and regulatory genetic elements. Transgenic murine models can have multiple copies of transgenes, abnormal expression of polyglutamine repeat-containing proteins, and transgene expression is not regulated by sequences that normally control the pattern and level of expression. Transgenic models provide considerable insight into the general processes causing neurodegeneration but may not be close mimics of specific human CAG repeat disorders. Knockin models of HD, SCA1, and SCA7 exhibit somewhat different phenotypes than seen in transgenic lines (Burright et al., 1995; Mangiarini et al., 1996; La Spada et al., 2001; Lin et al., 2001; Watase et al., 2002; Wheeler et al., 2002; Yoo et al., 2003). Whereas knockin lines require very long repeat numbers to produce a phenotype and the phenotype may be less aggressive than seen in transgenic lines, the patterns of pathology in knockin lines seem more similar to the human diseases. Important factors influencing phenotype in murine genetic models of HD are the number of repeats and the level of expression of mutant protein (see discussion above; Zoghbi and Botas, 2002). Knockin lines may have the virtue of disentangling the roles of repeat number and level of protein expression. In knockin lines, levels of expression are comparable from line to line and differences in phenotype can be attributed to differences in repeat number.

If transcriptional dysregulation is at the heart of pathogenesis in polyglutamine disorders, then transgenic models with heightened levels of protein expression and nonphysiological distributions of gene expression may give misleading impressions of key factors in the pathogenesis of regional neurodegeneration. Comparison of CRX protein activity in transgenic and knockin models of SCA7 suggests that the diminished CRX protein activity found in the transgenic model may be an artifact of abnormally regulated expression of SCA7 mutant protein in the transgenic model (La Spada et al., 2001; Yoo et al., 2003). Specific patterns of neurodegeneration may result from neuron subpopulation-specific interactions between expanded polyglutamine-containing protein fragments and transcriptionally active proteins, and these specific patterns of interaction may be distorted in transgenic models. At least with respect to HD, however, the more aggressive phenotypes exhibited by transgenic models are advantageous for some purposes. Evaluating potential therapies is easier in models with aggressive, early-onset phenotypes, and it will be prohibitively expensive to evaluate all potential therapies in HD knockin models. For all polyglutamine disorders, a combination of results from both transgenic and knockin models will likely be needed to investigate pathogenesis and evaluate potential therapies. $Hprt^{(CAG)146}$ mice may be particularly useful in this context. The wide expression of neuronal pathology in this line allows study of polyglutamine toxicity in many brain

regions with expression under the control of native elements.

LITERATURE CITED

Bazzett T, Albin RL. 2001. Huntington disease: a model excitotoxic chronic neurodegeneration. In: Palomo T, Beninger RJ, Archer T, editors. Neurodegenerative brain disorders. Madrid: Fundacion Cerebro y Mente. p 259–288.

Bazzett TJ, Falik RC, Becker JB, Albin RL. 1995. Chronic administration of malonic acid produces selective neural degeneration and transient changes in calbindin immunoreactivity in rat striatum. Exp Neurol 134:244–252.

Beal MF, Brouillet E, Jenkins B, Henshaw R, Rosen B, Hyman BT. 1993a. Age-dependent striatal excitotoxic lesions produced by the endogenous mitochondrial inhibitor malonate. J Neurochem 61:1147–1150.

Beal MF, Brouillet E, Jenkins BG, Ferrante RJ, Kowall NW, Miller JM, Storey E, Srivastava R, Rosen BR, Hyman BT. 1993b. Neurochemical and histologic characterization of striatal excitotoxic lesions produced by the mitochondrial toxin 3-nitropropionic acid. J Neurosci 13:4181–4192.

Becher MW, Kotzuk JA, Sharp AH, Davies SW, Bates GP, Price DL, Ross CA. 1998. Intranuclear neuronal inclusions in Huntington's disease and dentatorubral and pallidoluysian atrophy: correlation between the density of inclusions and IT15 CAG triplet repeat length. Neurobiol Dis 4:387–397.

Bogdanov MB, Ferrante RJ, Kuemmerle S, Klivenyi P, Beal MF. 1998. Increased vulnerability to 3-nitropropionic acid in an animal model of Huntington's disease. J Neurochem 71:2642–2644.

Boutell JM, Thomas P, Neal JW, Weston VJ, Duce J, Harper PS, Jones AL. 1999. Aberrant interactions of transcriptional repressor proteins with the Huntington's disease gene product, huntingtin. Hum Mol Genet 8:1647–1655.

Browne SE, Bowling AC, MacGarvey U, Baik MJ, Berger SC, Muqit MM, Bird ED, Beal MF. 1997. Oxidative damage and metabolic dysfunction in Huntington's disease: selective vulnerability of the basal ganglia. Ann Neurol 41:646–653.

Burright EN, Clark HB, Servadio A, Matilla T, Feddersen RM, Yunis WS, Duvick LA, Zoghbi HY, Orr HT. 1995. SCA1 transgenic mice: a model for neurodegeneration caused by an expanded CAG trinucleotide repeat. Cell 82:937–948.

Cha JH, Kosinski CM, Kerner JA, Alsdorf SA, Mangiarini L, Davies SW, Penney JB, Bates GP, Young AB. 1998. Altered brain neurotransmitter receptors in transgenic mice expressing a portion of an abnormal human huntington disease gene. Proc Natl Acad Sci U S A 95:6480–6485.

Chai Y, Wu L, Griffin JD, Paulson HL. 2001. The role of protein composition in specifying nuclear inclusion formation in polyglutamine disease. J Biol Chem 276:44889–44897.

Chai Y, Shao J, Miller VM, Williams A, Paulson HL. 2002. Live-cell imaging reveals divergent intracellular dynamics of polyglutamine disease proteins and supports a sequestration model of pathogenesis. Proc Natl Acad Sci U S A 99:9310–9315.

Cummings CJ, Reinstein E, Sun Y, Antalffy B, Jiang Y, Ciechanover A, Orr HT, Beaudet AL, Zoghbi HY. 1999. Mutation of the E6-AP ubiquitin ligase reduces nuclear inclusion frequency while accelerating polyglutamine-induced pathology in SCA1 mice. Neuron 24:879–892.

Davies SW, Turmaine M, Cozens BA, DiFiglia M, Sharp AH, Ross CA, Scherzinger E, Wanker EE, Mangiarini L, Bates GP. 1997. Formation of neuronal intranuclear inclusions underlies the neurological dysfunction in mice transgenic for the HD mutation. Cell 90:537–548.

DiFiglia M, Sapp E, Chase KO, Davies SW, Bates GP, Vonsattel JP, Aronin N. 1997. Aggregation of huntingtin in neuronal intranuclear inclusions and dystrophic neurites in brain. Science 277:1990–1993.

Dragatsis I, Levine MS, Zeitlin S. 2000. Inactivation of Hdh in the brain and testis results in progressive neurodegeneration and sterility in mice. Nat Genet 26:300–306.

Dunah AW, Jeong H, Griffin A, Kim YM, Standaert DG, Hersch SM, Mouradian MM, Young AB, Tanese N, Krainc D. 2002. Sp1 and TAFII130 transcriptional activity disrupted in early Huntington's disease. Science 296:2238–2243.

Dyer RB, McMurray CT. 2001. Mutant protein in Huntington disease is resistant to proteolysis in affected brain. Nat Genet 29:270–278.

Ferrante RJ, Andreassen OA, Dedeoglu A, Ferrante KL, Jenkins BG, Hersch SM, Beal MF. 2002. Therapeutic effects of coenzyme Q10 and remacemide in transgenic mouse models of Huntington's disease. J Neurosci 22:1592–1599.

Ferrer I, Goutan E, Marin C, Rey MJ, Ribalta T. 2000. Brain-derived neurotrophic factor in Huntington disease. Brain Res 866:257–261.

Fujigasaki H, Martin JJ, De Deyn PP, Camuzat A, Deffond D, Stevanin G, Dermaut B, Van Broeckhoven C, Durr A, Brice A. 2001. CAG repeat expansion in the TATA box-binding protein gene causes autosomal dominant cerebellar ataxia. Brain 124:1939–1947.

Goldberg YP, Nicholson DW, Rasper DM, Kalchman MA, Koide HB, Graham RK, Bromm M, Kazemi-Esfarjani P, Thornberry NA, Vaillancourt JP, Hayden MR. 1966. Cleavage of huntingtin by apopain, a proapoptotic cystein protease, is modulated by the polyglutamine tract. Nat Genet 13:380–382.

Gouw LG, Digre KB, Harris CP, Haines JH, Ptacek LJ. 1994. Autosomal dominant cerebellar ataxia with retinal degeneration: clinical, neuropathologic, and genetic analysis of a large kindred. Neurology 44:1441–1447.

Greene JG, Greenamyre JT. 1995. Characterization of the excitotoxic potential of the reversible succinate dehydrogenase inhibitor malonate. J Neurochem 64:430–436.

Guidetti P, Charles V, Chen EY, Reddy PH, Kordower JH, Whetsell WO Jr, Schwarcz R, Tagle DA. 2001. Early degenerative changes in transgenic mice expressing mutant huntingtin involve dendritic abnormalities but no impairment of mitochondrial energy production. Exp Neurol 169: 340–350.

Hansson O, Petersen A, Leist M, Nicotera P, Castilho RF, Brundin P. 1999. Transgenic mice expressing a Huntington's disease mutation are resistant to quinolinic acid-induced striatal excitotoxicity. Proc Natl Acad Sci U S A 96:8727–8732.

Hansson O, Castilho RF, Korhonen L, Lindholm D, Bates GP, Brundin P. 2001a. Partial resistance to malonate-induced striatal cell death in transgenic mouse models of Huntington's disease is dependent on age and CAG repeat length. J Neurochem 78:694–703.

Hansson O, Guatteo E, Mercuri NB, Bernardi G, Li XJ, Castilho RF, Brundin P. 2001b. Resistance to NMDA toxicity correlates with appearance of nuclear inclusions, behavioral deficits and changes in calcium homeostasis in mice transgenic for exon 1 of the Huntington gene. Eur J Neurosci 14:1492–1504.

Hickey MA, Reynolds GP, Morton AJ. 2002. The role of dopamine in motor symptoms in the R6/2 transgenic mouse model of Huntington's disease. J Neurochem 81:46–59.

Higgins DS, Greenamyre JT. 1996. [^{3}H]dihydrorotenone binding to NADH: ubiquinone reductase (complex I) of the electron transport chain: an autoradiographic study. J Neurosci 16:3807–3816.

Hodgson JG, Agopyan N, Gutekunst CA, Leavitt BR, LePiane F, Singaraja R, Smith DJ, Bissada N, McCutcheon K, Nasir J, Jamot L, Li XJ, Stevens ME, Rosemond E, Roder JC, Phillips AG, Rubin EM, Hersch SM, Hayden MR. 1999. A YAC mouse model for Huntington's disease with full-length mutant huntingtin, cytoplasmic toxicity, and selective striatal neurodegeneration. Neuron 23:181–192.

Holbert S, Denghien I, Kiechle T, Rosenblatt A, Wellington C, Hayden MR, Margolis RL, Ross CA, Dausset J, Ferrante RJ, Neri C. 2001. The Gln-Ala repeat transcriptional activator CA150 interacts with huntingtin: neuropathologic and genetic evidence for a role in Huntington's disease pathogenesis. Proc Natl Acad Sci U S A 98:1811–1816.

Holmberg M, Duyckaerts C, Durr A, Cancel G, Gourfinkel-An I, Damier P, Faucheux B, Trottier Y, Hirsch EC, Agid Y, Brice A. 1998. Spinocerebellar ataxia type 7 (SCA7): a neurodegenerative disorder with neuronal intranuclear inclusions. Hum Mol Genet 7:913–918.

Huntington's Disease Collaborative Research Group. 1993. A novel gene containing a trinucleotide repeat that is expanded and unstable on Huntington's disease chromosomes. Cell 72:971–983.

Huntington Study Group. 2001. A randomized, placebo-controlled trial of coenzyme Q10 and remacemide in Huntington's disease. Neurology 57:397–404.

Hurlbert MS, Zhou W, Wasmeier C, Kaddis FG, Hutton JC, Freed CR. 1999. Mice transgenic for an expanded CAG repeat in the Huntington's disease gene develop diabetes. Diabetes 48:649–651.

Huynh DP, Figueroa K, Hoang N, Pulst SM. 2000. Nuclear localization or inclusion body formation of ataxin-2 are not necessary for SCA2 pathogenesis in mouse or human. Nat Genet 26:44–50.

Iizuka R, Hirayama K. 1986. Dentato-rubro-pallido-luysian atrophy. In: Vinken PJ, Brurn GW, Klawans HL, editors. Handbook of clinical neurology 49. Amsterdam: Elsevier. p 437–444.

Ikeda H, Yamaguchi M, Sugai S, Aze Y, Narumiya S, Kakizuka A. 1996.

Expanded polyglutamine in the Machado-Joseph disease protein induces cell death in vitro and in vivo. Nat Genet 13:196–202.

Jen JC. 2003. Spinocerebellar ataxia 2 (SCA2). In: Pulst S-M, editor. Genetics of movement disorders. Amsterdam: Academic Press. p 81–84.

Jenkins BG, Koroshetz WJ, Beal MF, Rosen BR. 1993. Evidence for impairment of energy metabolism in vivo in Huntington's disease using localized 1H NMR spectroscopy. Neurology 43:2689–2695.

Jinnah HA, Gage FH, Friedmann T. 1991. Amphetamine-induced behavioral phenotype in a hypoxanthine-guanine phosphoribosyltransferase-deficient mouse model of Lesch-Nyhan syndrome. Behav Neurosci 105: 1004–1012.

Jinnah HA, Langlais PJ, Friedmann T. 1992. Functional analysis of brain dopamine systems in a genetic mouse model of Lesch-Nyhan syndrome. J Pharmacol Exp Ther 263:596–607.

Jinnah HA, Wojcik BE, Hunt M, Narang N, Lee KY, Goldstein M, Wamsley JK, Langlais PJ, Friedmann T. 1994. Dopamine deficiency in a genetic mouse model of Lesch-Nyhan disease. J Neurosci 14:1164–1175.

Katsuno M, Adachi H, Kume A, Li M, Nakagomi Y, Niwa H, Sang C, Kobayashi Y, Doyu M, Sobue G. 2002. Testosterone reduction prevents phenotypic expression in a transgenic mouse model of spinal and bulbar muscular atrophy. Neuron 35:843–854.

Kegel KB, Meloni AR, Yi Y, Kim YJ, Doyle E, Cuiffo BG, Sapp E, Wang Y, Qin ZH, Chen JD, Nevins JR, Aronin N, DiFiglia M. 2002. Huntingtin is present in the nucleus, interacts with the transcriptional corepressor C-terminal binding protein, and represses transcription. J Biol Chem 277:7466–7476.

Kim M, Lee HS, LaForet G, McIntyre C, Martin EJ, Chang P, Kim TW, Williams M, Reddy PH, Tagle D, Boyce FM, Won L, Heller A, Aronin N, DiFiglia M. 1999. Mutant huntingtin expression in clonal striatal cells: dissociation of inclusion formation and neuronal survival by caspase inhibition. J Neurosci 19:964–973.

Kim YJ, Yi Y, Sapp E, Wang Y, Cuiffo B, Kegel KB, Qin ZH, Aronin N, DiFiglia M. 2001. Caspase 3-cleaved N-terminal fragments of wild-type and mutant huntingtin are present in normal and Huntington's disease brains, associate with membranes, and undergo calpain-dependent proteolysis. Proc Natl Acad Sci U S A 98:12784–12789.

Klement IA, Skinner PJ, Kaytor MD, Yi H, Hersch SM, Clark HB, Zoghbi HY, Orr HT. 1998. Ataxin-1 nuclear localization and aggregation: role in polyglutamine-induced disease in SCA1 transgenic mice. Cell 95:41–53.

Kuemmerle S, Gutekunst CA, Klein AM, Li XJ, Li SH, Beal MF, Hersch SM, Ferrante RJ. 1999. Huntington aggregates may not predict neuronal death in Huntington's disease. Ann Neurol 46:842–849.

La Spada AR, Fu YH, Sopher BL, Libby RT, Wang X, Li LY, Einum DD, Huang J, Possin DE, Smith AC, Martinez RA, Koszdin KL, Treuting PM, Ware CB, Hurley JB, Ptacek LJ, Chen S. 2001. Polyglutamine-expanded ataxin-7 antagonizes CRX function and induces cone-rod dystrophy in a mouse model of SCA7. Neuron 31:913–927.

Levine MS, Klapstein GJ, Koppel A, Gruen E, Cepeda C, Vargas ME, Jokel ES, Carpenter EM, Zanjani H, Hurst RS, Efstratiadis A, Zeitlin S, Chesselet MF. 1999. Enhanced sensitivity to N-Methyl-D-aspartate receptor activation in transgenic and knockin mouse models of Huntington's disease. J Neurosci Res 58:515–532.

Li H, Li SH, Johnston H, Shelbourne PF, Li XJ. 2000. Amino-terminal fragments of mutant huntingtin show selective accumulation in striatal neurons and synaptic toxicity. Nat Genet 25:385–389.

Lin X, Antalffy B, Kang D, Orr HT, Zoghbi HY. 2000. Polyglutamine expansion down-regulates specific neuronal genes before pathologic changes in SCA1. Nat Neurosci 3:157–163.

Lin CH, Tallaksen-Greene S, Chien WM, Cearley JA, Jackson WS, Crouse AB, Ren S, Li XJ, Albin RL, Detloff PJ. 2001. Neurological abnormalities in a knock-in mouse model of Huntington's disease. Hum Mol Genet 10:137–144.

Luthi-Carter R, Strand A, Peters NL, Solano SM, Hollingsworth ZR, Menon AS, Frey AS, Spektor BS, Penney EB, Schilling G, Ross CA, Borchelt DR, Tapscott SJ, Young AB, Cha JH, Olson JM. 2000. Decreased expression of striatal signaling genes in a mouse model of Huntington's disease. Hum Mol Genet 9:1259–1271.

Mangiarini L, Sathasivam K, Seller M, Cozens B, Harper A, Hetherington C, Lawton M, Trottier Y, Lehrach H, Davies SW, Bates GP. 1996. Exon 1 of the HD gene with an expanded CAG repeat is sufficient to cause a progressive neurological phenotype in transgenic mice. Cell 87:493–506.

Mastroberardino PG, Iannicola C, Nardacci R, Bernassola F, De Laurenzi V, Melino G, Moreno S, Pavone F, Oliverio S, Fesus L, Piacentini M. 2002. "Tissue" transglutaminase ablation reduces neuronal death and prolongs survival in a mouse model of Huntington's disease. Cell Death Differ 9:873–880.

McCampbell A, Taylor JP, Taye AA, Robitschek J, Li M, Walcott J, Merry D, Chai Y, Paulson H, Sobue G, Fischbeck KH. 2000. CREB-binding protein sequestration by expanded polyglutamine. Hum Mol Genet 9:2197–2202.

McCampbell A, Taye AA, Whitty L, Penney E, Steffan JS, Fischbeck KH. 2001. Histone deacetylase inhibitors reduce polyglutamine toxicity. Proc Natl Acad Sci U S A 98:15179–15184.

Menalled LB, Sison JD, Wu Y, Oliveri M, Li X-J, Li H, Chesselet MF. 2002. Early motor dysfunction and striosomal distribution of huntington microaggregates in Huntington's disease knock-in mice. J Neurosci 22:8266–8276.

Nucifora FC Jr, Sasaki M, Peters MF, Huang H, Cooper JK, Yamada M, Takahashi H, Tsuji S, Troncoso J, Dawson VL, Dawson TM, Ross CA. 2001. Interference by huntingtin and atrophin-1 with CBP-mediated transcription leading to cellular toxicity. Science 291:2423–2428.

Ordway JM, Tallaksen-Greene S, Gutekunst CA, Bernstein EM, Cearley JA, Wiener HW, Dure LS, Lindsey R, Hersch SM, Jope RS, Albin RL, Detloff PJ. 1997. Ectopically expressed CAG repeats cause intranuclear inclusions and a progressive late onset neurological phenotype in the mouse. Cell 91:753–763.

Ordway JM, Cearley JA, Detloff PJ. 1999. CAG-polyglutamine-repeat mutations: independence from gene context. Philos Trans R Soc Lond B Biol Sci 354:1083–1088.

Panov AV, Gutekunst CA, Leavitt BR, Hayden MR, Burke JR, Strittmater WJ, Greenamyre JT. 2002. Early mitochondrial calcium defects in Huntington's disease are a direct effect of polyglutamines. Nat Neurosci 5:731–736.

Paulson HL, Perez MK, Trottier Y, Trojanowski JQ, Subramony SH, Das SS, Vig P, Mandel JL, Fischbeck KH, Pittman RN. 1997. Intranuclear inclusions of expanded polyglutamine protein in spinocerebellar ataxia type 3. Neuron 19:333–344.

Perutz MF, Johnson T, Suzuki M, Finch JT. 1994. Glutamine repeats as polar zippers: their possible role in inherited neurodegenerative diseases. Proc Natl Acad Sci U S A 91:5355–5358.

Pulst S-M. 2003. Spinocerebellar ataxia 2 (SCA2). In: Pulst S-M, editor. Genetics of movement disorders. Amsterdam: Academic Press. p 45–56.

Reddy PH, Williams M, Charles V, Garrett L, Pike-Buchanan L, Whetsell WO Jr, Miller G, Tagle DA. 1998. Behavioural abnormalities and selective neuronal loss in HD transgenic mice expressing mutated full-length HD cDNA. Nat Genet 20:198–202.

Reynolds GP, Dalton CF, Tillery CL, Mangiarini L, Davies SW, Bates GP. 1999. Brain neurotransmitter deficits in mice transgenic for the Huntington's disease mutation. J Neurochem 72:1773–1776.

Richfield EK, Young AB, Penney JB. 1989. Comparative distributions of dopamine D-1 and D-2 receptors in the cerebral cortex of rats, cats, and monkeys. J Comp Neurol 286:409–426.

Robitaille Y, Schut L, Kish SJ. 1995. Structural and immunocytochemical features of olivopontocerebellar atrophy caused by the spinocerebellar ataxia type 1 (SCA-1) mutation define a unique phenotype. Acta Neuropathol (Berl) 90:572–581.

Ross CA. 1997. Intranuclear neuronal inclusions: a common pathogenic mechanism for glutamine-repeat neurodegenerative diseases? Neuron 19:1147–1150.

Ross CA. 2002. Polyglutamine pathogenesis: emergence of unifying mechanisms for Huntington's disease and related disorders. Neuron 35:819–822.

Rubinsztein DC, Leggo J, Coles R, Almqvist E, Biancalana V, Cassiman JJ, Chotai K, Connarty M, Crauford D, Curtis A, Curtis D, Davidson MJ, Differ AM, Dode C, Dodge A, Frontali M, Ranen NG, Stine OC, Sherr M, Abbott MH, Franz ML, Graham CA, Harper PS, Hedreen JC, Jackson A, Kaplan JC, Losekoot M, MacMillan JC, Morrison P, Trottier Y, Novelletto A, Simpson S, Theilman J, Whittaker JL, Folstein SE, Ross CA, Hayden MR. 1996. Phenotypic characterization of individuals with 30–40 CAG repeats in the Huntington disease (HD) gene reveals HD cases with 36 repeats and apparently normal elderly individuals with 36–39 repeats. Am J Hum Genet 59:16–22.

Rubinsztein DC, Leggo J, Chiano M, Dodge A, Norbury G, Rosser E, Craufurd D. 1997. Genotypes at the GluR6 kainate receptor locus are associated with variation in the age of onset of Huntington disease. Proc Natl Acad Sci U S A 94:3872–3876.

Sanchez I, Mahlke C, Yuan J. 2003. Pivotal role of oligomerization in expanded polyglutamine neurodegenerative disorders. Nature 421: 373–378.

Sathasivam K, Hobbs C, Turmaine M, Mangiarini L, Mahal A, Bertaux F, Wanker EE, Doherty P, Davies SW, Bates GP. 1999. Formation of polyglutamine inclusions in non-CNS tissue. Hum Mol Genet 8:813–822.

Sato K, Kashihara K, Okada S, Ikeuchi T, Tsuji S, Shomori T, Morimoto K, Hayabara T. 1995. Does homozygosity advance the onset of dentatorubral-pallidoluysian atrophy? Neurology 45:1934–1936.

Sato T, Oyake M, Nakamura K, Nakao K, Fukusima Y, Onodera O, Igarashi S, Takano H, Kikugawa K, Ishida Y, Shimohata T, Koide R, Ikeuchi T, Tanaka H, Futamura N, Matsumura R, Takayanagi T, Tanaka F, Sobue G, Komure O, Takahashi M, Sano A, Ichikawa Y, Goto J, Kanazawa I. 1999. Transgenic mice harboring a full-length human mutant DRPLA gene exhibit age-dependent intergenerational and somatic instabilities of CAG repeats comparable with those in DRPLA patients. Hum Mol Genet 8:99–106.

Saudou F, Finkbeiner S, Devys D, Greenberg ME. 1998. Huntingtin acts in the nucleus to induce apoptosis but death does not correlate with the formation of intranuclear inclusions. Cell 95:55–66.

Sawa A, Wiegand GW, Cooper J, Margolis RL, Sharp AH, Lawler JF, Greenamyre JT, Snyder SH, Ross CA. 1999. Increased apoptosis of Huntington disease lymphoblasts associated with repeat length-dependent mitochondrial depolarization. Nat Med 5:1194–1198.

Shelbourne PF, Killeen N, Hevner RF, Johnston HM, Tecott L, Lewandoski M, Ennis M, Ramirez L, Li Z, Iannicola C, Littman DR, Myers RM. 1999. A Huntington's disease CAG expansion at the murine Hdh locus is unstable and associated with behavioural abnormalities in mice. Hum Mol Genet 8:763–774.

Scherzinger E, Lurz R, Turmaine M, Mangiarini L, Hollenbach B, Hasenbank R, Bates GP, Davies SW, Lehrach H, Wanker EE. 1997. Huntingtin-encoded polyglutamine expansions form amyloid-like protein aggregates in vitro and in vivo. Cell 90:549–558.

Schilling G, Becher MW, Sharp AH, Jinnah HA, Duan K, Kotzuk JA, Slunt HH, Ratovitski T, Cooper JK, Jenkins NA, Copeland NG, Price DL, Ross CA, Borchelt DR. 1999. Intranuclear inclusions and neuritic aggregates in transgenic mice expressing a mutant N-terminal fragment of huntingtin. Hum Mol Genet 8:397–407.

Shimohata T, Nakajima T, Yamada M, Uchida C, Onodera O, Naruse S, Kimura T, Koide R, Nozaki K, Sano Y, Ishiguro H, Sakoe K, Ooshima T, Sato I, Ikeuchi T, Oyake M, Sato T, Aoyagi Y, Hozumi I, Nagatsu T, Takiyama Y, Nishizawa M, Goto J, Kanazawa I, Davidson I, Tanese N, Takahashi H, Tsuji S. 2000. Expanded polyglutamine stretches interact with TAFII130, interfering with CREB-dependent transcription. Nat Genet 26:29–36.

Simeoni S, Mancini MA, Stenoien DL, Marcelli M, Weigel NL, Zanisi M, Martini L, Poletti A. 2000. Motoneuronal cell death is not correlated with aggregate formation of androgen receptors containing an elongated polyglutamine tract. Hum Mol Genet 9:133–144.

Sisodia SS. 1998. Nuclear inclusions in glutamine repeat disorders: are they pernicious, coincidental, or beneficial? Cell 95:1–4.

Sobue G, Doyu M, Nakao N, Shimada N, Mitsuma T, Maruyama H, Kawakami S, Nakamura S. 1996. Homozygosity for Machado-Joseph disease gene enhances phenotypic severity. J Neurol Neurosurg Psychiatry 60:354–356.

Squitieri F, Gellera C, Cannella M, Mariotti C, Cislaghi G, Rubinsztein DC, Almqvist EW, Turner D, Bachoud-Levi AC, Simpson SA, Delatycki M, Maglione V, Hayden MR, Di Donato S. 2003. Homozygosity for CAG mutation in Huntington disease is associated with a more severe clinical course. Brain 4:946–955.

Steffan JS, Kazantsev A, Spasic-Boskovic O, Greenwald M, Zhu YZ, Gohler H, Wanker EE, Bates GP, Housman DE, Thompson LM. 2000. The Huntington's disease protein interacts with p53 and CREB-binding protein and represses transcription. Proc Natl Acad Sci U S A 97:6763–6768.

Steffan JS, Bodai L, Pallos J, Poelman M, McCampbell A, Apostol BL, Kazantsev A, Schmidt E, Zhu YZ, Greenwald M, Kurokawa R, Housman DE, Jackson GR, Marsh JL, Thompson LM. 2001. Histone deacetylase inhibitors arrest polyglutamine-dependent neurodegeneration in Drosophila. Nature 413:739–743.

Stine OC, Pleasant N, Franz ML, Abbott MH, Folstein SE, Ross CA. 1993. Correlation between the onset age of Huntington's disease and length of the trinucleotide repeat in IT-15. Hum Mol Genet 2:1547–1549.

Suzuki M, Desmond TJ, Albin RL, Frey KA. 2001. Vesicular neurotransmitter transporters in Huntington's disease: initial observations and comparison with traditional synaptic markers. Synapse 41:329–336.

Tabrizi SJ, Workman J, Hart PE, Mangiarini L, Mahal A, Bates G, Cooper JM, Schapira AH. 2000. Mitochondrial dysfunction and free radical damage in the Huntington R6/2 transgenic mouse. Ann Neurol 47:80–86.

Takiyama Y, Oyanagi S, Kawashima S, Sakamoto H, Saito K, Yoshida M, Tsuji S, Mizuno Y, Nishizawa M. 1994. A clinical and pathologic study of a large Japanese family with Machado-Joseph disease tightly linked to the DNA markers on chromosome 14q. Neurology 44:1302–1308.

Takeyama K, Ito S, Yamamoto A, Tanimoto H, Furutani T, Kanuka H, Miura M, Tabata T, Kato S. 2002. Androgen-dependent neurodegeneration by polyglutamine-expanded human androgen receptor in Drosophila. Neuron 35:855–864.

Taylor JP, Hardy J, Fischbeck KH. 2002. Toxic proteins in neurodegenerative disease. Science 296:1991–1995.

Tellez-Nagel I, Johnson AB, Terry RD. 1974. Studies on brain biopsies of patients with Huntington's chorea. J Neuropathol Exp Neurol 33:308–332.

Trojanowski JQ, Lee VM. 2000. "Fatal attractions" of proteins. A comprehensive hypothetical mechanism underlying Alzheimer's disease and other neurodegenerative disorders. Ann N Y Acad Sci 924:62–67.

Vander Borght TM, Sima AAF, Kilbourn MR, Desmond TJ, Kuhl DE, Frey KA. 1995a. [^{3}H]Methoxytetrabenazine: a high specific activity ligand for estimating monoaminergic neuronal integrity. Neuroscience 68: 955–962.

Vander Borght T, Kilbourn M, Desmond T, Kuhl D, Frey K. 1995b. The vesicular monoamine transporter is not regulated by dopaminergic drug treatments. Eur J Pharmacol 294:577–583.

Watase K, Weeber EJ, Xu B, Antalffy B, Yuva-Paylor L, Hashimoto K, Kano M, Atkinson R, Sun Y, Armstrong DL, Sweatt JD, Orr HT, Paylor R, Zoghbi HY. 2002. A long CAG repeat in the mouse Sca1 locus replicates SCA1 features and reveals the impact of protein solubility on selective neurodegeneration. Neuron 34:905–919.

Wellington CL, Ellerby LM, Hackam AS, Margolis RL, Trifiro MA, Singaraja R, McCutcheon K, Salvesen GS, Propp SS, Bromm M, Rowland KJ, Zhang T, Rasper D, Roy S, Thornberry N, Pinsky L, Kakizuka A, Ross CA, Nicholson DW, Bredesen DE, Hayden MR. 1998. Caspase cleavage of gene products associated with triplet expansion disorders generates truncated fragments containing the polyglutamine tract. J Biol Chem 273:9158–9167.

Wellington CL, Ellerby LM, Gutekunst CA, Rogers D, Warby S, Graham BK, Loubser O, van Raamsdonk J, Singajara R, Yang YZ, Gafni J, Bedesen D, Hersch SM, Leavitt BR, Roy S, Nicholson DW, Hayden MR. 2002. Caspase cleavage of mutant huntingtin precedes neurodegeneration in Huntington's disease. J Neurosci 22:7862–7872.

Wexler NS, Young AB, Tanzi RE, Travers H, Starosta-Rubinstein S, Penney JB, Snodgrass SR, Shoulson I, Gomez F, Ramos Arroyo MA, Penchaszadeh GK, Moreno H, Gibbins K, Faryniarz A, Hobbs W, Anderson MA, Bonilla E, Conneally PM, Gusella JF. 1987. Homozygotes for Huntington's disease. Nature 326:194–197.

Wheeler VC, White JK, Gutekunst CA, Vrbanac V, Weaver M, Li XJ, Li SH, Yi H, Vonsattel JP, Gusella JF, Hersch S, Auerbach W, Joyner AL, MacDonald ME. 2000. Long glutamine tracts cause nuclear localization of a novel form of huntingtin in medium spiny striatal neurons in HdhQ92 and HdhQ111 knock-in mice. Hum Mol Genet 9:503–513.

Wheeler VC, Gutekunst CA, Vrbanac V, Lebel LA, Schilling G, Hersch S, Friedlander RM, Gusella JF, Vonsattel JP, Borchelt DR, MacDonald ME. 2002. Early phenotypes that presage late-onset neurodegenerative disease allow testing of modifiers in Hdh CAG knock-in mice. Hum Mol Genet 11:633–640.

Yang Q, Hashizume Y, Yoshida M, Wang Y, Goto Y, Mitsuma N, Ishikawa K, Mizusawa H. 2000. Morphological Purkinje cell changes in spinocerebellar ataxia type 6. Acta Neuropathol (Berl) 100:371–376.

Yoo S-Y, Pennesi ME, Weeber EJ, Xu B, Atkinson R, Chen S, Armstrong DL, Wu SM, Sweatt JD, Zogbhi HY. 2003. SCA7 knockin mice model human SCA7 and reveal gradual accumulation of mutant ataxin-7 in neurons and abnormalities in short-term plasticity. Neuron 37:383–401.

Zeron MM, Hansson O, Chen N, Wellington CL, Leavitt BR, Brundin P, Hayden MR, Raymond LA. 2002. Increased sensitivity to N-methyl-D-aspartate receptor-mediated excitotoxicity in a mouse model of Huntington's disease. Neuron 33:849–860.

Zhang S, Xu L, Lee J, Xu T. 2002. Drosophila atrophin homolog functions as a transcriptional corepressor in multiple developmental processes. Cell 108:45–56.

Zoghbi H, Botas J. 2002. Mouse and fly models of neurodegeneration. Trends Genet 18:463.

Zuccato C, Ciammola A, Rigamonti D, Leavitt BR, Goffredo D, Conti L, MacDonald ME, Friedlander RM, Silani V, Hayden MR, Timmusk T, Sipione S, Cattaneo E. 2001. Loss of huntingtin-mediated BDNF gene transcription in Huntington's disease. Science 293:493–498.